

Mutation in Arabidopsis mitochondrial pentatricopeptide repeat 40 gene affects tolerance to water deficit.

Ph.D. Dissertation

Kamal Kant

Supervisor: Dr. Zsigmond Laura



Doctoral School of Biology

University of Szeged

Institute of Plant Biology,

HUN-REN Biological Research Centre, Szeged

Szeged, 2024

Table of Contents

List of Abbreviations:.....	4
1. Introduction	6
1.1 <i>Arabidopsis thaliana</i> as a model plant	7
1.2.1 Drought stress.....	8
1.2.2 Plant responses to drought stress.....	9
1.2.3 ABA stomata relation and ABA signaling	9
1.3 Mitochondria and stress.....	10
1.3.1 Alternative oxidases	12
1.4 PPR protein family	12
1.4.1 Characterization of the <i>ppr40</i> mutant.....	14
2. Objectives.....	20
3. Research Methodology.....	21
3.1 Plant material and growth conditions	21
3.2 Drought assay/survival assay	21
3.3 Stomata conductance	22
3.3 Chlorophyll fluorescence measurement	22
3.4 Relative water content	22
3.5 Proline estimation.....	23
3.6 Lipid peroxidation assay	24
3.7 RNA Extraction and qPCR analysis.....	24
3.8 Metabolomics	25
3.9 Plant phenotyping.....	26
3.10 Software tools and statistical analysis	28
4. Results	29
4.1 Evaluation of drought tolerance	29
4.2 Confirmation of drought tolerance in <i>ppr40</i> mutants through plant phenotyping.....	30
4.3 Confirmation of drought tolerance in <i>ppr40</i> mutants through physiological parameters..	36
4.4 Stomatal conductance patterns in <i>ppr40-1</i> mutant highlight ABA hypersensitivity and altered responses to water stress.....	39
4.5 Insights from a metabolomics survey under water stress conditions	39
4.6 Enhanced stability of photosynthesis in drought-stressed <i>ppr40</i> mutants.....	41
4.7 Oxidative damage is alleviated by <i>ppr40</i> mutations	44
4.8 Modulation of drought-induced gene expression by <i>PPR40</i>	46
4.9 Hormone signaling modulation under drought stress.....	48
5. Discussion	51
6. Summary	56
7. Összefoglaló	59

9. References	63
10. List of publications: (MTMT: 10074888)	72
11. Declaration	73
12. Supplementary data	74

List of Abbreviations:

ABA – Abscisic Acid

ABF – ABRE-Binding factor

ABO5 – ABA-Overly Sensitive 5

ABRE - Abscisic acid-responsive elements

AHG11 - ABA Hypersensitive Germination 11

AOX – Alternative Oxidases

APX – Ascorbate Peroxidase

COI1 – Coronatine Insensitive 1

EIN3 – Ethylene Insensitive 3

ETC – Electron Transport Chain

MDA - Malonaldehyde

NPR1- Non-expressor PR genes 1

OsNBL3 – *Oryza sativa* Natural Blight Leaf 3

P5CS - Δ^1 -Pyrroline-5-carboxylate synthase

PAM – Pulse amplitude modulation

PDH – Proline Dehydrogenase

PGN – PPR Protein for Germination on NaCl

PIPs - Plasma membrane intrinsic proteins

PPR – Pentatricopeptide repeat

PSII – Photosystem II

QY Max – Maximum Quantum Yield

RAB18 – Responsive to ABA 18

RD29A – Responsive to dessication 29A

ROS – Reactive Oxygen Species

RWC – Relative Water Content

SLG1 – Slow Growth 1

SLO2 – Slow Growth 2

SOAR1 - Suppressor of the ABAR-overexpressor 1

SOL – Slenderness of Leaves

SVR7 – Suppressor of Variegation 7

TBA- Thiobarbituric Acid

TCA – Thiochloroacetic acid

1. Introduction

Climate change in recent years caused compounding and cascading risks to the environment. In the summer of 2022, Europe encountered a striking drought of a magnitude not observed in the past 500 years. The simultaneous effect of exceptionally high temperatures and minimal precipitation resulted in river depletion, wildfires, and the exacerbation of crop failures. Simultaneously, the western regions of the United States faced the most severe drought conditions in the last 1200 years, while specific stretches of the Yangtze River in China, which is known as the country's longest river, experienced historically low water levels since at least 1865, primarily due to extreme temperatures and a profound deficiency of rainfall. (Wang et al. 2023)

Climate change, with its far-reaching consequences, poses a formidable threat to our environment and the delicate balance of ecosystems. Droughts have triggered a series of environmental disasters, including river depletion, rampant wildfires, and devastating crop failures (Orimoloye et al. 2022). The impact of climate change is felt acutely by sessile organisms, particularly plants, which play a critical role in global food production.

Transpiration, regulated by the stoma on leaf surfaces, and the presence of a thick cuticle layer on dermal tissues are essential mechanisms that plants employ to conserve water. However, in the face of more frequent and severe droughts, these natural defenses are proving inadequate. As a result, the agricultural sector, which heavily relies on the health and productivity of plants, faces unprecedented challenges in sustaining global food production. Feeding a projected population of 9.8 billion people by 2050 is a daunting task, particularly in drought-prone and arid regions of the developing world (He et al. 2019).

In recent decades, significant progress has been made in increasing global food production to meet the demands of a growing population. However, climate change poses an existential threat to these achievements, placing immense strain on food security in vulnerable regions. Sub-Saharan Africa regularly experiences droughts that hinder agricultural productivity, leading to food shortages and economic hardship. The situation is further exacerbated by other climatic variables such as heatwaves, floods, and conflicts, which compound the challenges faced by farmers and governments in these regions (Tamasiga et al. 2023).

Food production shocks, characterized by sudden and unexpected losses in agricultural yield and fluctuations in food prices, have become increasingly common in various sectors during the last five decades. Extreme weather events account for half of these shocks,

disproportionately affecting countries with limited coping capabilities. Farmers in these regions often struggle to diversify their food production, while governments find it difficult to import food or provide insurance to mitigate the impacts of climate-induced crises. A stark example of the dire consequences of climate change-induced droughts is the 2017 Kenya drought, which plunged the nation into a state of national emergency, leaving approximately 2.5 million people hungry and vulnerable. The frequency and intensity of droughts are projected to increase due to climate change, necessitating urgent action to implement more effective adaptation methods and innovative sustainable practices (Uhe et al. 2018).

To address the challenges posed by climate change and secure food production in drought-prone regions, it is imperative to focus on sustainable adaptation strategies. These strategies should prioritize enhancing the resilience of agricultural systems to withstand extreme weather events. Emphasis must be placed on research and development efforts that promote drought-resistant crop varieties, water-efficient irrigation techniques, and environmentally conscious farming practices.

In conclusion, climate change-induced droughts pose a significant threat to food security, particularly in vulnerable regions with limited coping capabilities. The intensifying impact of extreme weather events necessitates immediate action to develop and implement sustainable adaptation methods in agriculture. By investing in resilient agricultural practices and fostering innovation, we can strive towards a more food-secure future in the face of a changing climate. The urgency of this matter calls for collective efforts from governments, researchers, farmers, and global communities to secure the sustenance and well-being of future generations.

1.1 *Arabidopsis thaliana* as a model plant

Arabidopsis thaliana, commonly referred to as thale cress, is a medium-sized flowering plant belonging to the *Brassicaceae* family. It holds significant importance as a model organism for studying plant genetics. This versatile plant is closely related to economically valuable crops like rapeseed, cabbage, and broccoli, making it a valuable research tool for dicotyledonous weed species within the *Brassicaceae* family.

Arabidopsis possesses numerous favorable characteristics for laboratory investigations. Its life cycle, encompassing seed germination, rosette plant formation, flowering, and seed maturation, occurs astonishingly fast, completing within a short six-week period (Meinke et al. 1998). It exhibits self-compatibility, produces a high yield of seeds per generation, and showcases desirable traits for a model plant in laboratory settings. With a small genome size of approximately 135 megabase pairs (Mbp) and a chromosome count of $2n=10$, *Arabidopsis* is

well-suited for genetic, biochemical, and physiological studies. The Arabidopsis genome contains relatively few repetitive DNA sequences: 10-14% of the total DNA (including nuclear, mitochondrial, and chloroplast DNA) is highly repetitive, 23-27% is moderately repetitive, and 50-55% consists of unique copies (Meyerowitz 1992). Additionally, a wide range of ecotypes collected from natural populations provides researchers with ample material for experimental analysis.

In the year 2000, the complete sequencing of Arabidopsis thaliana's genome, comprising five pairs of chromosomes, was successfully achieved (The Arabidopsis Genome Initiative, 2000). This breakthrough enabled a comprehensive exploration of its genetic composition. This wealth of genetic information offers invaluable insights into the functioning of Arabidopsis and serves as a foundation for investigating gene functions in other dicotyledonous plants.

Arabidopsis's amenability to genetic manipulation has made it a powerful platform for research. Numerous T-DNA insertion mutants have been generated, greatly facilitating investigations into the roles of diverse genes in Arabidopsis (Koncz et al., 1992; Szabados et al., 2002; Alonso et al., 2003). This vast collection of mutants opens avenues for studying gene functions and their potential applications in other plant species. Genes isolated from Arabidopsis can be utilized for the study of similar genes in other plants or directly applied in practical plant breeding. This allows for the relatively rapid application of findings from molecular biological research conducted on the Arabidopsis model in the fields of agriculture and industry.

1.2.1 Drought stress

Drought (water stress) is one of the most important environmental stresses and occurs because of low rainfall. Drought is a major problem faced by farmers every year. It is a natural phenomenon that is triggered and sustained over an extended period by the inadequate availability of freshwater for the needs of humans and the ecosystem (Ahluwalia et al. 2021a). Besides affecting food production, drought reduces underground water levels, deteriorates water quality, increases soil erosion, and can eventually result in other calamities like fire, floods, and spread of diseases (Ahluwalia et al. 2021b). According to the United Nations World Water Development Report 2018, an estimated 55 million people are affected worldwide due to drought and about 700 million people are at risk of being displaced by 2030 because of it (World Water Assessment Report).

1.2.2 Plant responses to drought stress

Drought leads to multidimensional stress and causes changes in the physiological, morphological, biochemical, and molecular traits in plants (Salehi-Lisar and Bakhshayeshan-Agdam 2016). Mechanisms such as photosynthesis and gas exchange (Menezes-Silva et al. 2017; Bryant et al. 2021), cell death, changes in cell wall composition, nutrient translocation (Demidchik 2015), transcriptional activity of genes, transposable elements (Makarevitch et al. 2015), lipid signaling (Hou et al. 2016), metabolites, proteins (Nakabayashi and Saito 2015) and antioxidant profile (Choudhury et al. 2017) can be altered during stress. Plants must recognize and respond to stress conditions with a variety of biological signals at appropriate times and speeds for their survival (Takahashi and Shinozaki 2019). Higher plants achieve sophisticated responses and adaptations to abiotic stresses, including drought, to maintain optimal growth under stress conditions. For these complex physiological responses in plants, a variety of cellular and molecular regulatory mechanisms are required for short-term responses to prevent water loss via transpiration from guard cells and for long-term adaptations to acquire stress resistance at the whole-plant level (Nakashima et al. 2014; Takahashi et al. 2018). Some mechanisms like production of reactive oxygen species (ROS) such as singlet oxygen, superoxide, hydroxyl radicals and hydrogen peroxide (H₂O₂) are a consequence of abiotic stresses such as drought, salinity, heavy metals, high light or high temperature. ROS can damage proteins, lipids, and other macromolecules and therefore create additional oxidative stress for the plants. ROS are however not only damaging compounds but play essential signaling roles in hormonal regulation during plant development, activating cellular defenses and stress response. (Considine and Foyer 2014; You and Chan 2015; Mullineaux et al. 2018).

The drought stress responses of vascular plants are complex regulatory mechanisms because they include various physiological responses from signal perception under water deficit conditions to the acquisition of drought stress resistance at the whole-plant level. It is thought that plants first recognize water deficit conditions in roots and that several molecular signals then move from roots to shoots (Takahashi et al. 2020).

1.2.3 ABA stomata relation and ABA signaling

During drought stress, the coordination of phytohormones and reactive oxygen species (ROS) assumes a pivotal role. These phytohormones, including auxins (Cheol Park et al. 2013), gibberellins (GA) (Gaion and Carvalho 2021), cytokinins (Prerostova et al. 2018), salicylic acid (SA) (Farooq et al. 2009), ethylene (Zhu et al. 2018), jasmonates (JA) (Riemann et al.

2015), and brassinosteroids (BRs) (Chen et al. 2017), orchestrate a wide array of adaptive mechanisms that enable plants to thrive under challenging conditions. Among them, abscisic acid (ABA) stands out as a key player. When drought stress sets in, ABA levels surge, triggering a cascade of protective responses. These responses include the activation of stress-responsive genes (Li et al. 2018; Chen et al. 2021b), forming a complex gene regulatory network that equips plants to combat environmental challenges (Nakashima et al., 2014, Takahashi et al., 2018).

These mechanisms encompass the control of stomatal aperture and the expression of genes that confer resistance to environmental stresses (Lim et al. 2015).

Intriguingly, some of the secondary messengers triggered by ABA can also play roles in plants' adaptation to both abiotic and biotic stress. Notable examples include ROS, nitric oxide (NO), and cytosolic free Ca^{2+} (León et al. 2014; Huang et al. 2019). These secondary messengers participate in intricate signaling networks that aid plants in their resilience against stressors.

In both biotic and abiotic stresses, ROS emerges as key actors in plant defense mechanisms. These ROS, including superoxide radicals, hydrogen peroxide (H_2O_2), and NO (He et al. 2007; Daszkowska-Golec and Szarejko 2013), are by-products of aerobic metabolism. Furthermore, when drought stress looms, ABA accumulation is primarily increase within the leaves' vasculature because almost all ABA biosynthesis enzymes are expressed in vascular tissues (Finkelstein 2013, Kuromori et al. 2018)

When it comes to coping with drought stress, the regulation of stomatal closure is a critical mechanism for water conservation. This process involves the activation of outward K^+ channels, which results in a reduction of water potential within guard cells. Therefore, water is expelled from the guard cells, leading to decreased turgor pressure and eventual stomatal closure (Munemasa et al. 2015). Moreover, the involvement of guard cell aquaporins in the regulation of stomatal aperture has been suggested. Among these, plasma membrane-intrinsic proteins (PIPs) serve as major facilitators, allowing the diffusion of water across the plasma membrane (Maurel et al. 2016).

1.3 Mitochondria and stress

Plant mitochondria typically appear as spherical or rod-shaped organelles within the range of 1–3 μm in length and approximately 0.5 μm in diameter, with each plant cell containing several hundreds of these vital organelles (Logan 2006). Mitochondria, integral to cellular

function, exhibit a dynamic and pleomorphic nature, featuring a smooth outer membrane enveloping an inner membrane with a significantly larger surface area. The inner membrane surrounds a protein-rich core known as the matrix (Leaver et al. 1983; Gray et al. 1999). Mitochondria are semi-autonomous, possessing their own genetic material and protein-synthesizing machinery. A substantial portion of mitochondrial polypeptides is encoded in the nuclear genome, synthesized in the cytosol, and subsequently imported into the mitochondria post-transcriptionally (Unsold et al. 1997; Whelan and Glaser 1997; Duby and Boutry 2002).

The mitochondrial electron transport chain and Fo-F1 ATP synthase, often collectively referred to as the respiratory chain, are a series of protein complexes in the inner mitochondrial membrane (IMM) that play central roles in oxidative phosphorylation. In oxidative phosphorylation system (OXPHOS), electrons are extracted from metabolic pathways involving carbohydrates, fatty acids, and amino acids, and are then transferred to the mitochondrial electron transport chain (mETC). As electrons are passed along the chain to the final electron acceptor, oxygen protons are pumped across the inner mitochondrial membrane (IMM). The resulting proton gradient is then used by Fo-F1 ATP synthase to produce ATP (Maclean et al. 2022).

Complexes I and II transfer electrons to ubiquinone, a mobile electron transporter within the inner mitochondrial membrane. Ubiquinol, the reduced form of ubiquinone, transfers electrons to Complex III. Electron transport from complex III to Complex IV is mediated by cytochrome c, a small and hydrophilic protein localized in the mitochondrial intermembrane space. The OXPHOS comprises all the components of the electron transport chain (mETC) and the ATP synthase complex, which, strictly speaking, is not part of the ETC but is designated as complex V (Braun 2020). This highly conserved process occurs in the mitochondria of animals, fungi and plants. However, in plants, oxidative phosphorylation (OXPHOS) occurs within the framework of photosynthesis and various stress response reactions (Millar et al. 2011a; Schertl and Braun 2014). Plant mitochondria is tightly connected with several metabolic and catabolic processes for example ascorbate biosynthesis, proline degradation, TCA cycle. Mitochondria contain complete TCA cycle as they are able to oxidize most of the respiratory substrates. (Møller et al. 2021)

Leaf mitochondria play a crucial role in mitigating environmental stresses by modulating cell redox homeostasis and influencing antioxidant capacity (Dutilleul et al. 2003). Additionally,

plant mitochondria may serve as early sensors of cellular stress, regulating programmed cell death (Jones 2000; Rhoads et al. 2006).

1.3.1 Alternative oxidases

In plant mitochondria, when the main electron transport pathway (cytochrome *c* pathway) is damaged or blocked through the electron transport chain (ETC), the alternative oxidases (AOX) can help to remove accumulated excess electrons. Alternative oxidases are potentially ‘energy wasteful’ protein that dramatically reduces ATP generation, with most of the energy dissipated as heat, and avoid the formation of reactive oxygen species by preventing over-reduction of the electron transport chain (Selinski et al. 2018).

There are two terminal oxidases in the plant mitochondrial ETC. One is the usual cytochrome (cyt) oxidase (complex IV), and the other one is the AOX (Selinski et al. 2018). AOX liberates the highly coupled and extreme electron transport processes in mitochondria, thereby supplying and maintaining much-needed metabolic homeostasis by directly reducing oxygen to water (Saha et al. 2016).

In *Arabidopsis*, the AOX gene family consists of five members: Aox1a, 1b, 1c, 1d, and 2. Each of these genes is active, but there are noticeable variations in their expression patterns across different organs and developmental stages. This suggests that they might have slightly different biological functions (Clifton et al. 2006). Interestingly, some of the AOX genes rank among the most responsive to stress in *Arabidopsis* (Møller et al. 2021). Alternative oxidases prove to be a key player in helping plants cope with various environmental challenges such as drought, intense light, salinity, and heavy metal stress. When the AOX genes are highly expressed, they can boost the plant's ability to withstand abiotic stress, through the regulation of ROS generation and the safeguarding of the photosystem (Zhang et al. 2012).

1.4 PPR protein family

The family of PPR (pentatricopeptide repeat) proteins is a group of proteins that are found in plants. They are characterized by 9-15 repeated units of pentatricopeptide domains and short segments of 35 conserved amino acids. These repeated units form a helical structure and are responsible for binding to RNA molecules. PPR domains share similarities with tetratricopeptide repeats (TPR), which are involved in protein-protein interactions, suggesting that PPR segments may also have the ability to bind to other proteins. In plants, the PPR protein family is relatively large, with 441 members identified in *Arabidopsis thaliana*, with all described proteins localized to mitochondria or, chloroplast, or nucleus (Small and Peeters

2000; Lurin et al. 2004a; Schitzlinneweber and Small 2008). However, the exact biological roles of most PPR proteins are still not fully understood.

PPR proteins are classified into two groups, namely P and PLS, based on the types of motifs they contain and how these motifs are arranged. P-class proteins exclusively feature canonical P-motifs, each consisting of 35 amino acids. On the other hand, PLS-class proteins are more diverse, incorporating P-motifs (35 amino acids), L-motifs (35 or 36 amino acids), and S-motifs (31 or 32 amino acids) arranged in tandem to form PLS triplets (Lurin et al. 2004). Within the PLS class, proteins often have carboxyl-terminal extensions that include highly conserved E, E+, or DYW domains (Cheng et al. 2016).

PPR proteins play important roles in regulating gene expression in mitochondria through post-transcriptional processes. They are involved in various aspects of RNA metabolism within mitochondria (Salone et al. 2007), including RNA editing (Ichinose et al. 2012; Hayes and Santibanez 2020), splicing (Hashimoto et al. 2003), cleavage, translation initiation, and association with ribosomes. In some cases, they also help anchor translation complexes to the inner membrane of mitochondria, facilitating the integration of newly synthesized proteins into the appropriate complexes.

They play a role in RNA maturation processes such as capping, nucleotide modifications, methylation, polyadenylation, and RNA segment excision and ligation. By controlling RNA metabolism and translation, PPR proteins regulate gene expression in organelles (Liu et al. 2013, Zhang and Lu 2019). Additionally, PPR genes have been found to influence various biological processes in plants, including cytoplasmic male sterility, circadian clock function, and seed development. Mutations in PPR genes can lead to detrimental effects such as embryo lethality, reduced fertility, and dwarf phenotypes, highlighting their crucial roles in plant growth and development.

Being one of the largest gene families, PPR proteins exhibit diverse functions in controlling metabolism and signaling within organelles. Some of these proteins influence key signaling pathways, including ABA and ethylene, which impact how plants respond to abiotic stresses like drought (Yuan and Liu 2012; Zhu et al. 2014).

One remarkable PPR protein called SOAR1 localizes in both the cytosol and nucleus, and its involvement in ABA signaling greatly contributes to the plant's ability to endure drought, salt, and cold stress (Jiang et al. 2015; Lu et al. 2022). Another important member, GENOMES

UNCOUPLED 1 (GUN1), resides in the chloroplast and plays a vital role in retrograde signaling, essential for integrating developmental and stress-related signals (Koussevitzky et al. 2007). GUN1's function is crucial in safeguarding chloroplasts from oxidative stress, as evidenced by the *gun1* mutant displaying reduced activities of superoxide dismutase (SOD) and ascorbate peroxidase (APX), leading to higher levels of reactive oxygen species (ROS) and oxidative damage (Fortunato et al. 2022).

The mitochondrial PPR protein OsNBL3 in rice plays a pivotal role in *nad5* splicing and the activity of mitochondrial electron transport chain complex I. The *osnbl3* mutant showcases various significant effects, including elevated alternative respiration, growth retardation, wilting leaves, premature senescence, improved resistance against pathogens, and enhanced salt stress tolerance (Qiu et al. 2021). SVR7, found in chloroplasts, is involved in both photosynthesis and the plant's ability to tolerate oxidative stress (Lv et al. 2014). Furthermore, six mitochondrial PPR proteins in Arabidopsis, namely PPR40 (Zsigmond et al. 2008), ABO5 (Liu et al. 2010), AHG11 (Murayama et al. 2012), SLG1 (Yuan and Liu 2012), PGN (Laluk et al. 2011), and SLO2 (Zhu et al. 2014) have been shown to regulate ABA signaling and influence the plant's response to salt and drought stress. Interestingly, while mutants in these genes exhibit heightened sensitivity to salt or osmotic stress during germination and early growth stages, adult plants of the *slo2* or *slg1* mutants display increased drought and salt tolerance (Yuan and Liu 2012; Zhu et al. 2014). This suggests that these PPR proteins regulate plant responses to abiotic stresses depending on developmental stage. Their action possibly affects reactive oxygen species (ROS) homeostasis and mediates stress responses through modulation of ABA signaling. While most PPR proteins are in mitochondria or chloroplasts, only a few have been found in other cellular compartments, such as the cytosol or nucleus. Specifically, two PPR proteins found in the nucleus have been identified as regulators of embryogenesis (Ding et al. 2006; Hammani et al. 2011). However, to date, no PPR protein localized in the nucleus or cytosol has been discovered to directly regulate plant responses to abiotic stresses.

1.4.1 Characterization of the *ppr40* mutant

During the T-DNA insertion mutagenesis program (Szabados et al. 2002), a transgenic Arabidopsis line has been identified that exhibited increased sensitivity to abscisic acid (ABA) and reduced size (semi-dwarf phenotype) due to a mutation. Subsequent germination and growth assays revealed that the mutant plant was sensitive to ABA, sugar and salt. Based on the classification of Lurin et al. (2004), the mutant was named as *ppr40-1*. During the

characterization of the *ppr40-1* mutant, a tandem inverted (LB-RB/RB-LB) T-DNA insertion in the coding region of the *At3g16890* gene was found. The T-DNA insertion caused a 4-base pair deletion of 311 base pairs downstream of the ATG start codon in the 3' direction (Figure 1). Another allele was obtained from the SALK insertion mutant collection (<http://signal.salk.edu/cgi-bin/tdnaexpress>) and named *ppr40-2* (SALK_071712). In this mutant, the T-DNA insertion occurred 852 base pairs downstream of the ATG start codon in the 3' direction, causing a 5-base pair deletion. The *ppr40-1* mutant is a null phenotype, while *ppr40-2* displays a partially altered "leaky" phenotype likely due to truncated protein production.

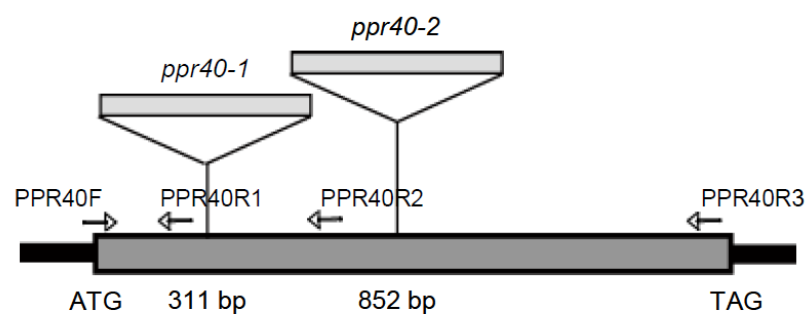


Figure 1: T-DNA insertion sites and gene-specific PCR primers in the *At3g16890* gene. The schematic representation illustrates the disruption of the *At3g16890* gene in the *ppr40-1* and *ppr40-2* alleles. In the *ppr40-1* allele, the coding sequence is interrupted by an inverted T-DNA repeat located 311 bp downstream of the ATG codon. Conversely, in the *ppr40-2* allele (SALK_071712), a T-DNA insertion occurs at position 852 bp downstream of the ATG codon (Zsigmond et al, 2008).

The *PPR40* gene (*At3g16890*) contains one exon, which is 1980 base pairs long. The gene encodes a protein of 659 amino acids with a molecular weight of 74.26 kDa. The PPR40 protein belongs to the P subclass of the PPR protein family (Lurin et al. 2004) and contains a predicted mitochondrial targeting signal and 14 conserved pentatricopeptide repeat motifs. The PPRs are separated into two domains (Figure 2).

The PPR domain protein PPR40 plays a crucial role in Complex III activity. Mutations in PPR40 lead to a reduction in the activity of Complex III, but not to a complete loss of activity. PPR40 is not itself a core subunit of complex III, although it is essential for the regulation of Complex III cytochrome c reductase activity. The mutations in *ppr40-1* and *ppr40-2* lead to probable truncated transcripts, resulting in proteins that are missing 9 or all the PPR repeats. In *ppr40-1* mutants, the defective cytochrome c pathway results in increased production of superoxide ions, which are then converted to H₂O₂ by MnSOD (Zsigmond et al. 2008).

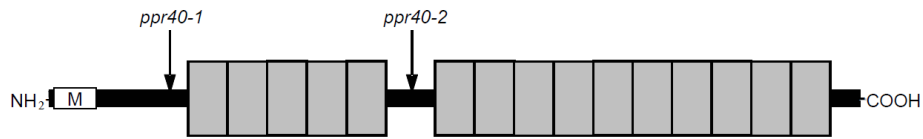


Figure 2: Domain architecture of the PPR40 protein. This diagram depicts the domain structure of the PPR40 protein, highlighting essential features. The mitochondrial targeting signal (mt) and two PPR repeat domains (5 × PPR, 9 × PPR) are indicated. Notably, arrows denote the termination points of PPR40 sequences in the predicted PPR40-1 and PPR40-2 proteins, providing insights into the disrupted regions caused by T-DNA insertions (Zsigmond et al, 2008).

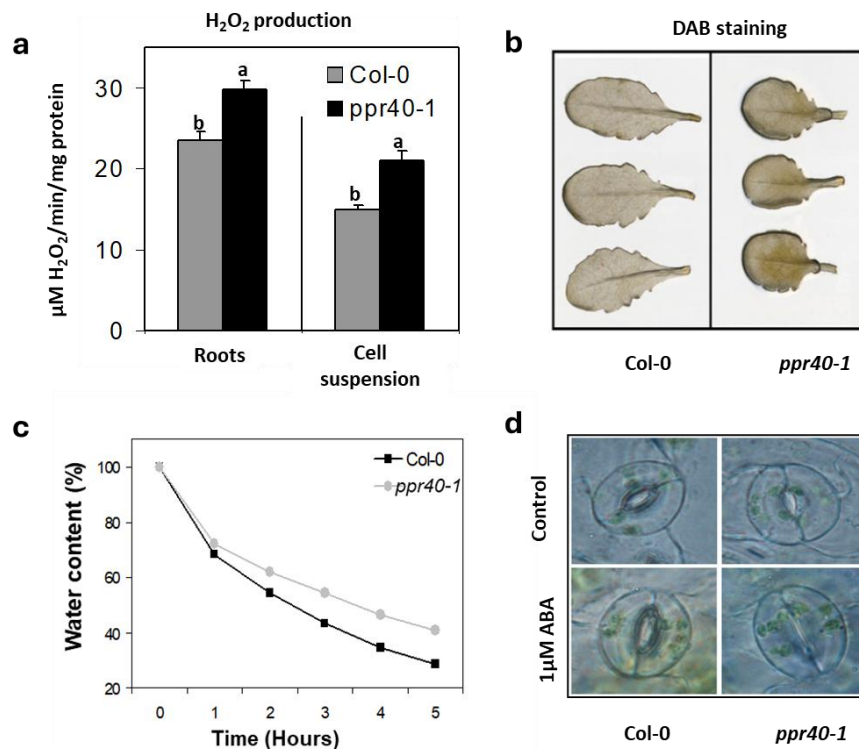


Figure 3: Responses of *ppr40-1* mutant compared to wild-type (Col-0) plants under various conditions. a) Production of H₂O₂ in roots and cell suspension in normal conditions. b) Detection of hydrogen peroxide in leaves of wild-type (Col-0) and *ppr40-1* plants by DAB histochemical assay. c) Water loss of detached leaves of wild-type (Col-0) and *ppr40-1* mutant plants. d) Enhanced stomatal closure in *ppr40-1* epidermal layers indicates enhanced ABA sensitivity (Zsigmond et al, 2008)

Reduced respiration in *ppr40-1* mutants results in an increased H₂O₂ generation in the mitochondria which can act as a signal for cellular defence responses. Reduced electron

transport by Complex III, resulting in increased use of alternative electron donors such as ascorbate by Complex IV. Mitochondrial defects leading to increased ROS generation and a possible limitation of ATP production might be responsible for the hypersensitivity of *ppr40-1* mutants to ABA and salt stress. On the other hand, in silico analysis did not reveal any known RNA-binding motif in PPR40, although other mitochondrial PPR proteins are involved in RNA processing and splicing (Zsigmond et al. 2008). Therefore, further studies are necessary to understand how PPR40 is involved in the regulation of Complex III through molecular interactions with its core subunits.

Based on the findings of Zsigmond et al. (2008), it was observed that the *ppr40-1* mutant maintained higher water content in a leaf desiccation experiment compared to the wild type. This suggests that the mutant may have mechanisms that allow it to conserve water more effectively under drought conditions. The enhanced stomatal closure observed in the *ppr40-1* mutant suggests that it may have an increased sensitivity or responsiveness to ABA and higher production of H₂O₂ because of compromised mETC which could confer improved drought tolerance (Figure 3). By focusing on this mutant in drought studies, there is an opportunity to elucidate the underlying genetic and molecular mechanisms that contribute to drought tolerance.

1.5 High throughput Plant Phenotyping

The HUN-REN Biological Research Centre, Szeged hosts a state-of-the-art plant phenotyping facility, which is instrumental in characterizing Arabidopsis plants. This facility employs a sophisticated setup for daily plant imaging. Overhead CCD cameras capture RGB images, and the entire process is seamlessly orchestrated within a PlantScreenTM analysis chamber. This chamber allows for automated plant transportation between imaging, weighing, and watering stations. The RGB images are captured simultaneously and are stored in a central database. To extract valuable data, these images undergo pre-processing, following the methodology outlined in (Awlia et al. 2016). This process enables the collection of both binary and RGB data for each plant. Binary images play a crucial role in calculating growth parameters, including area and perimeter. These parameters, comprising area, perimeter, and convex hull, are then harnessed for real-time calculations of various morphometric rosette parameters. These parameters include roundness, roundness 2, isotropy, eccentricity, compactness, rotational mass symmetry (RMS), and slenderness of leaves (SOL) (Figure 4) using the PlantScreenTM analyzer from PSI, Czech Republic.

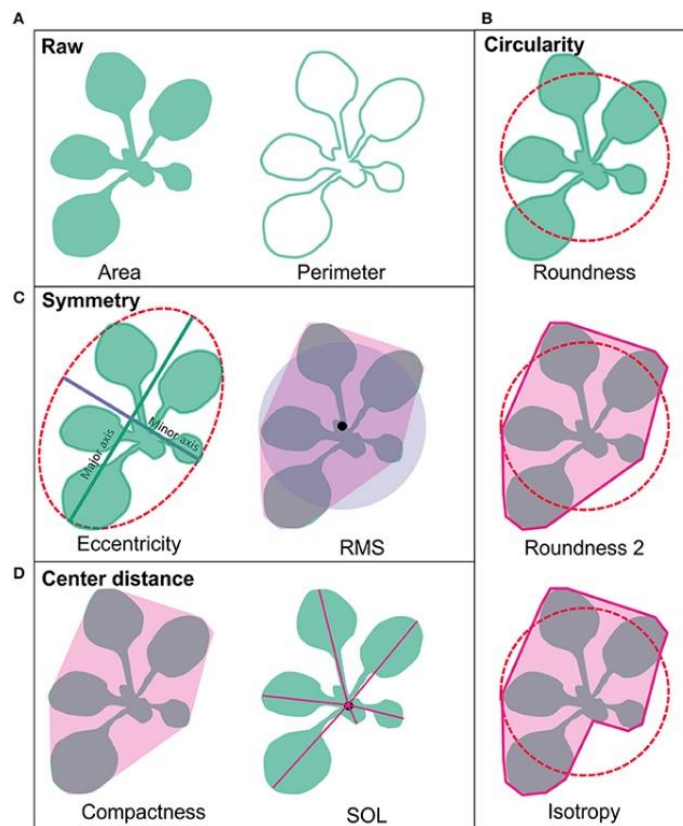


Figure 4: Rosette morphology parameters analysis. (A) Raw Parameters: Area and perimeter of the rosette are determined by counting pixels in binary images of the rosette and its edge pixels, respectively. The values are then converted to millimeters for quantification. (B) Circular Parameters: roundness, roundness 2, and isotropy are parameters reflecting circular characteristics of the rosette. (C) Symmetric Parameters: Eccentricity and RMS represent symmetric features of the rosette. (D) Center-Based Parameters: Compactness and SOL are calculated based on the center distance. The pink area surrounding RMS, compactness, and roundness 2 illustrates the rosette convex hull, while for isotropy, it represents the rosette polygon. (Source: Pavicic et al. 2017)

To characterize the overall morphology of the mutant lines, these nine morphological parameters (Figure 4) are grouped into four categories based on their characteristics: raw, circularity, symmetry, and center distance. Raw parameters, such as area and perimeter, are represented by measuring the number of pixels in a rosette picture and its edge pixels, which are then transformed into millimeters. The circularity parameters, including roundness, roundness 2, and isotropy, offer insights into the circular aspects of the rosette's shape. Roundness, in particular, describes the rosette area concerning a perfect circle with the same perimeter, considering factors like leaf slenderness and petiole length. Eccentricity and RMS provide information on the symmetry of the plant rosette, with eccentricity reflecting the

elliptical shape of the rosette and RMS indicating its overall symmetry. Compactness and SOL, on the other hand, are centered around center distance. Compactness expresses the ratio between the rosette area and the rosette convex hull area, shedding light on petiole length and leaf blade width. SOL, on the other hand, highlights the sharpness of leaf blades while being influenced by the number of leaves present (Pavicic et al. 2017).

2. Objectives

The general objective of the study was to investigate how *ppr40* mutants which affect mitochondrial electron transport influence responses to water deficit, and what is their role in modulating drought tolerance in model plant *Arabidopsis thaliana*.

Objectives of this study were as follows:

- Assess the survival rates of *ppr40-1*, *ppr40-2*, and Col-0 wild type plants during drought stress.
- Measure the physiological parameters including Electron Transport Rate, proline content, lipid peroxidation, and relative water content in *ppr40-1*, *ppr40-2*, and Col-0 plants under drought stress.
- Examine the expression levels of drought-related genes in *ppr40-1*, *ppr40-2*, and Col-0 plants under drought stress.
- Utilize advanced phenotyping system to evaluate leaf characteristics such as green area, compactness, area ratio, slenderness, and different PSII parameters (e.g. QY max) in *ppr40-1*, *ppr40-2*, and Col-0 plants under drought stress.

3. Research Methodology

3.1 Plant material and growth conditions

During our experiments, we worked with *Arabidopsis thaliana* Columbia-0 ecotype as a wild type, *PPR40* overexpression and the T-DNA insertion mutants *ppr40-1* (Zsigmond et al., 2008, 2012) and *ppr40-2* (*SALK_071712*). The T-DNA insertion mutants *ppr40-1* and *ppr40-2* of *Arabidopsis thaliana* with Col-0 background have previously been characterized (Zsigmond et al., 2008). Whereas *PPR40-OX* genotype was described in Zsigmond et al. (2012) The plants were grown in Plantobalt Substrate 1 sieved soil, approximately 30 grams in each pot.

(<https://www.plantaflor.de/en/products/propagation/details/plantobalt-substrate-1-fine-80-20-clay>). The experimental conditions maintained a constant temperature of 22 °C, an 8/16 h light/dark cycle, and an approximate photon flux density of 150 $\mu\text{mol m}^{-2} \text{s}^{-1}$.

3.2 Drought assay/survival assay

To conduct this investigation, plants were cultivated under standard growth conditions in growth chambers, maintained at a temperature. Concurrently, another set of plants was grown in a greenhouse, exposed to natural light conditions but maintaining the same temperature conditions as growth chambers. Plants were monitored and nurtured 21-35 days depending on conditions, ensuring optimal growth and health.

Following the initial growth period, drought stress was induced by withholding water from the plants for 7-14 days. This period of water deprivation aimed to simulate the adverse effects of prolonged drought conditions. After the stress period, the plants were re-watered and allowed to recover for 7 days under their respective growth conditions (growth chambers and greenhouse). The water deprived state of plants in growth chambers and green house was 14 days and 7 days respectively. The difference in the duration of water deprivation between the growth chamber and greenhouse experiments, due to the fluctuating humidity in the greenhouse causing more rapid drying, whereas the more controlled conditions in the growth chambers mean that plants take longer to dry. In addition, plants in both environments were selected for similar size and stage of development to minimise variability.

To evaluate the recovery rate, the number of healthy green plants were counted after the 7-day recovery period. By comparing the number of surviving plants with the initial population, the percentage of surviving plants in each condition was calculated. Statistical analyses were

conducted to assess any significant differences between the recovery rates in mutant and wild types.

3.3 Stomata conductance

Stomata conductance was measured in Col-0 and *ppr40-1* mutants using a LI-6400 Portable Photosynthesis System (LI-COR Environmental GmbH, Germany). This instrument is commonly employed in plant physiology studies. During the experiments, plants were maintained in a controlled environment. The relative humidity inside the growth chamber was set at 65 %. We ensured a constant flow rate of 300 μmol per second, and the block temperature was maintained at 23 °C throughout the experiments. To ensure consistent conditions for the plants, we kept the reference level of carbon dioxide (CO_2) at 400 parts per million (ppm) and the light intensity at 150 μmol per square meter per second. These parameters are crucial in maintaining a stable environment for plant measurements. Our measurements were taken at daily intervals following the cessation of irrigation. This allowed us to monitor how the plants' stomata conductance responded to changes in their water supply. We analyzed 15 plants for each genotype, ensuring a robust dataset for our research.

3.3 Chlorophyll fluorescence measurement

In this study, the evaluation of photosynthetic capacity was carried out by assessing various parameters using an Imaging-PAM system (M-Series, Maxi version; Heinz Walz GmbH), detailed in (Baker 2008). Before conducting the measurements, the plants were ensured to have adapted to darkness for 15 minutes.

The study evaluated the Electron Transport Rate (ETR), photosystem II (PSII) maximum quantum efficiency (F_v/F_m), and the quantum yield of PSII (Φ_{PSII}) as indicators of photosynthetic performance. A light curve approach was employed, which involved measuring fluorescence parameters at various photosynthetic photon flux densities. Specifically, measurements were taken at photon flux densities of 0, 55, 110, 185, 280, 335, and 395 μmol per square meter per second. For each plant, two distinct leaf areas were selected for assessment, ensuring robust data. To establish reliable results, measurements were conducted on a total of 15 plants for each genotype, and the entire experiment was repeated three times.

3.4 Relative water content

We assessed the relative water content (RWC) in plants subjected to different watering conditions, specifically well-watered and drought-treated plants, following the procedure

outlined by (Barrs and Weatherley 1962). To ensure robust and consistent results, fresh leaf tissue was collected from approximately 30 individual plants in each plant line.

The first step involved weighing the collected leaf samples (referred to as "W" in our calculations). Subsequently, to ensure full turgidity, the samples were hydrated by either floating them in de-ionized water or by hydrating them through the leaf petiole. This approach was chosen to minimize potential errors that can arise from variations in rehydration methods. After reaching full turgidity, the samples were gently dried to remove any surface moisture and then weighed to determine their full turgid weight (TW).

To obtain the dry weight (DW), the samples were subjected to oven-drying at approximately 80 °C and then weighed again. The RWC was calculated using the following formula: $RWC (\%) = [(W - DW) / (TW - DW)] \times 100$. This RWC measurement serves as a valuable indicator of the plant's water status and its ability to retain water under different conditions. To ensure the reliability of our findings, the experiment was conducted three times, providing a potent dataset for our analysis.

3.5 Proline estimation

Free proline content in plant samples was determined using a ninhydrin-based colorimetric assay, as described (Ábrahám et al. 2010). This method relies on the reaction of proline with ninhydrin, forming a colored reaction product that can be quantified spectrophotometrically. To begin the analysis, plant samples were collected from each genotype and treatment. Four replicates were prepared for each sample to ensure data accuracy and reproducibility. The absorbance of the reaction product was measured at a wavelength of 520 nm using the Thermo Scientific, Multiscan Go Microplate Spectrophotometer. To calculate the proline concentration in the plant samples, a standard curve was established using known concentrations of proline standards. These standards were subjected to the same ninhydrin-based colorimetric assay, and their absorbance values were measured at 520 nm using the microplate spectrophotometer. The resulting data were used to plot a standard curve, which allowed for the conversion of absorbance values of the unknown samples into proline concentrations. Once the absorbance values of the plant samples were obtained, they were correlated with the standard curve to determine their respective proline concentrations. Statistical analysis was performed to assess any significant differences in proline content between different genotypes and treatments. The experiments were repeated three times independently.

3.6 Lipid peroxidation assay

To evaluate lipid peroxidation, we employed the well-established thiobarbituric acid-reactive substances (TBARS) assay as described by (Heath and Packer 1968). 50-100 mg of leaf tissues from three biological replicates of all genotypes were homogenized in 1 ml of 0.1 % trichloroacetic acid (TCA). The homogenates were centrifuged at 13000 rpm for 20 minutes. 250 μ l of the supernatant was collected carefully and mixed with 1 ml of a reaction mixture (0.5 % thiobarbituric acid (TBA) and 20 % TCA). This mixture was incubated at 96 °C for 30 minutes. This will allow the reaction between TBA and malondialdehyde (MDA), a byproduct of lipid peroxidation. The absorbance of the resulting chromophore was measured at 532 nm using a Multiskan GO microplate reader (Thermo Fisher Scientific). To correct for nonspecific absorbance, a reference measurement was taken at 600 nm and subtracted from the absorbance at 532 nm.

To determine the concentration of MDA, which serves as a marker for lipid peroxidation, we utilized the extinction coefficient $\epsilon_{532} = 155 \text{ mM}^{-1} \text{ cm}^{-1}$. This coefficient allows the conversion of absorbance measurements into MDA concentration. The entire experiment was carried out with three biological replicates.

3.7 RNA Extraction and qPCR analysis

In this study, the extraction of total RNA was carried out using 100 mg of Arabidopsis leaves, following the protocol outlined by Yaffe et al. (2012). This method ensured the isolation of high-quality RNA. To eliminate any potential contamination with DNA, the extracted RNA underwent treatment with the TURBO DNA-free™ Kit, a product from Thermo Fisher Scientific known for effectively degrading DNA while preserving the integrity of the RNA molecules. For the subsequent step of complementary DNA (cDNA) synthesis, 1 μ g of the purified RNA was used. This transformation of RNA into cDNA was achieved through the utilization of the High-Capacity cDNA Reverse Transcription Kit, a product of Applied Biosystems. The reverse transcription process adhered to the manufacturer's recommendations, ensuring the efficient conversion of RNA into cDNA.

To conduct quantitative real-time polymerase chain reaction (qRT-PCR) experiments, an ABI 7900 Fast Real-Time System, manufactured by Applied Biosystems, was employed. The reaction mix utilized for these experiments consisted of SYBR Green qPCR Master Mixes from Thermo Scientific, which facilitated specific and sensitive gene amplification. To determine the relative transcript levels of the target genes, suitable reference genes were used for normalization. The choice of the reference genes *UBC18* (*AT5G42990*) and *ACT2*

(*AT3G18780*) was made based on their proven stability in expression across various experimental conditions.

For the analysis of the qRT-PCR data, the $2^{-\Delta Ct}$ or $2^{-\Delta\Delta Ct}$ method was applied. This method is described by (Livak and Schmittgen 2001),

3.8 Metabolomics

We analyzed the metabolic profiles of the Col-0 and *ppr40-1* mutant plants, which were subjected to water deprivation stress. To do this, 50 milligrams of leaf material from 4-week-old plants were collected, weighed, and frozen in liquid nitrogen. Subsequently, the frozen samples were grounded using an MM400 laboratory mill from Retsch, Germany, operating at 30 Hz for 1 minute. Following homogenization, the samples were resuspended in an extraction buffer composed of 40 % methanol, 20 % water, and 40 % acetonitrile. For each 30 milligrams of leaf material, 1 milliliter of the extraction buffer was added and vigorously vortexed the samples for 10 minutes. The next step involved centrifugation at 20000 g, maintained at 4 °C for 10 minutes, after which the supernatant was collected.

For metabolomic analysis, an ultrahigh-performance liquid chromatography-tandem mass spectrometry (UPLC-MS/MS) system was employed, specifically the Thermo Q-Exactive Focus instrument from Thermo Fisher Scientific in the USA, equipped with a Dionex Unimate 3000 UHPLC system. An Xbridge Premier BEH Amide column (2.1 mm × 150 mm, 2.5 μm) from Waters Corporation for chromatographic separation was utilized. Five microliters of each sample were injected into the system. The mobile phase composition was gradually altered from 98% solvent A (a mixture of 97.5 % acetonitrile and 2.5 % water) to 80 % solvent B (a combination of 20 % acetonitrile and 20 mM ammonium acetate + 20 mM ammonia in water) over a span of 9 minutes. This was carried out using a flow rate of 400 μL/min and a gradient profile 6. After a 1-minute equilibration period, the eluent composition returned to its initial conditions within 0.5 minutes, and the system was equilibrated for 4 minutes. For the acquisition of semi-quantitative metabolome data, the system operated in MS1 scan mode with negative ionization. The data were acquired with specific settings: sheath gas at 55 l/min, auxiliary gas at 14 l/min, sweep gas at 4 l/min, probe heater at 440 °C, capillary temperature at 280 °C, and a capillary voltage of 2500 V in negative ionization mode. Scanning mass ranged from 80 to 800 m/z with an automatic gain control (AGC) target of 3×10^6 and a maximum ion trap (IT) time of 250 ms. Pooled extract samples as quality controls were also used, injecting multiple times throughout the batch following established guidelines.

For the identification and verification of metabolites, 6 preselected compounds, pooled from the extracts, were injected multiple times at the end of the sequence. To acquire MS2 data, we used different normalized collision energies (NCE) of 10, 30, and 50 for data-dependent mass spectrometry (DDMS) confirmation mode.

Data processing and analysis involved using Tracefinder to obtain peak intensity values. The signal intensities (peak area) were extracted for 37 putatively identified metabolite signals based on retention time (± 0.25 minutes) and exact mass data (± 5 ppm). Metabolite data were subjected to PQN normalization, and we selected 6 metabolites for MS2 level confirmation. For putative metabolite identification at the MS2 level, Compound Discoverer 2.1 was used and searched against the Endogenous Metabolites compound class of the mzCloud database. The metabolites presented in this study were identified at the highest available level A (Alseekh et al. 2021).

To assess the statistical significance of our findings, ANOVA analysis was performed using the aov function from the stats package. For data visualization and analysis, we utilized tidyverse (Wickham et al. 2019) and ggplot (Wickham and Wickham 2016). All statistical and normalization procedures were carried out using the R statistical language, specifically version 4.0. Furthermore, all data generated from this study will be made accessible in the MetaboLights repository. This ensures transparency and allows for further validation and exploration of the results.

3.9 Plant phenotyping

In this study, the phenotypic responses of the wild-type Col-0 plants and two mutant lines, *ppr40-1* and *ppr40-2*, were investigated using the advanced PlantScreen™ Compact System from Photon System Instrument (PSI). To ensure consistency and comparability with previous research, we followed the experimental protocol established by (Faragó et al. 2022).

The plants were cultivated in individual pots containing Plantobalt Substrate 1 soil, which is renowned for promoting optimal plant growth. To maintain controlled environmental conditions, we implemented an 8-hour light and 16-hour dark cycle (short day conditions), with temperatures ranging between 22 °C during the day and 20 °C at night. A relative humidity of 65 % was also upheld. Illumination was provided by LEDs emitting a combination of cool white light (5700 K), deep red light (660 nm, 30 %), blue light (470 nm, 20 %), far-red light (740 nm, 30 %), and ultraviolet (UV) light (405 nm, 20 %), resulting in a photon irradiance of

130 μmol per square meter per second. These conditions were carefully optimized to ensure the best possible growth environment for the plants.

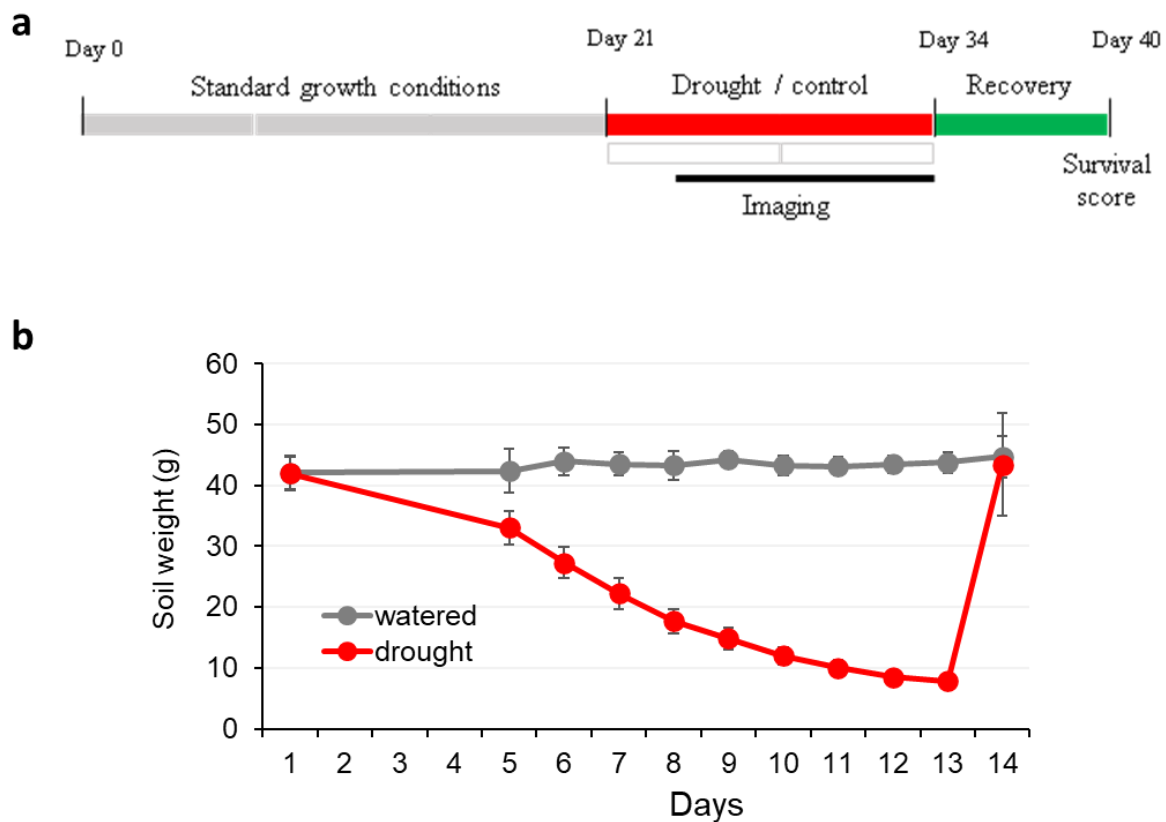


Figure 5: Illustration of the phenotyping experimental design for the drought study. a) Sequence of plant growth and treatments. Plants were grown in standard conditions for 21 days, then watering was stopped for 13 days. Plant recovery was stimulated by rewatering at day 34. b) Change of soil water content in the stress period. Gray line indicates weight change of well-watered pots (watered). Red line shows changes of pots after watering was stopped (drought).

The experimental duration comprised two main phases: the growth phase and the stress induction phase. During the initial 21 days after sowing, the plants were allowed to establish stable growth and development. Following this period, drought stress was induced by withholding water for 13 days, subjecting the plants to challenging conditions. Subsequently, a recovery phase was initiated by rewatering the plants, enabling us to assess their capacity to recuperate after enduring water stress. Throughout the drought stress period, daily imaging of the plants was conducted (Figure 5). This involved using a top-view RGB GigE PSI RGB camera with a high resolution of 12.36 MP. In addition to RGB images, chlorophyll fluorescence (ChlF) images were captured using the FluorCam FC-800MF Pulse Amplitude-modulated (PAM) system. The PAM system employed pulse-modulated short-duration measuring flashes with red-orange 620 nm light at 33 μs for F_0 , 800 ms of saturation pulses

with cool-white light at 1200 μmol per square meter per second irradiance in the dark-adapted state for Fm, and 180-second intervals of cool-white actinic light at 130 μmol per square meter per second.

For this study, a total of 40 plants were analyzed for each genotype and treatment, ensuring robust statistical power. Data processing and retrieval of raw data were facilitated by the PlantScreen™ Data Analyzer software provided by PSI. To ensure data quality, a rigorous curation process was applied to identify and eliminate any outliers from the dataset. The curated dataset was then subjected to a statistical analysis, which involved analysis of variance (ANOVA) with the Kruskal–Wallis test, followed by pairwise Wilcoxon's test or Mann–Whitney's test of significance (with a significance level of $p < 0.05$). These statistical analyses adhered to the methodology outlined by (Julkowska et al. 2019).

3.10 Software tools and statistical analysis

All the data analyses were implemented using the software Rstudio (RStudio Team (2020). RStudio: Integrated Development for R. RStudio, PBC, Boston, MA URL <http://www.rstudio.com/>), Origin (2020b) version 9.7.5.184 (Academic) and Microsoft Excel (2016).

We conducted the experiments with a minimum of three to four independent biological repetitions to ensure the reliability of our results. The data presented are expressed as the mean \pm standard error (SE), which was calculated by combining the data from these independent repetitions. To determine significant differences from the wild-type control, we employed Student's t-test (significant differences were denoted as * for $p \leq 0.05$, ** for $p \leq 0.01$, and *** for $p \leq 0.001$), and ANOVA with Tukey test or Fisher's LSD test.

4. Results

4.1 Evaluation of drought tolerance

ABA sensitivity of the *ppr40* mutants was determined in germination assays (Zsigmond et al. 2008). The *ppr40-1* knockout mutant exhibited a pronounced ABA hypersensitivity, with significantly delayed germination compared to the wild-type Col-0 plants. On the other hand, the *ppr40-2* knockdown mutant displayed an intermediate level of ABA sensitivity, indicating partial impairment of ABA responses. While *ppr40* mutants showed sensitivity to salt, the overexpression line of *PPR40* displayed enhanced tolerance to salt and reduced oxidative damage (Zsigmond et al. 2012).

To evaluate the consequences of altered ABA responses in drought conditions, survival rates of the *ppr40* mutants and Col-0 wild-type plants were compared after exposure to water stress. Following the re-watering phase, surviving *ppr40-1* mutants quickly resumed turgor and displayed a green rosette after a few days, indicating successful recovery. In contrast, the dead plants, including Col-0 and *ppr40-2* mutants, exhibited chlorosis, signifying irreversible damage due to prolonged water stress (Figure 6).

After 12 days of water deprivation, the *ppr40-1* mutant showed a significantly higher percentage of surviving plants compared to Col-0 (Figure 7), suggesting a greater level of drought tolerance. The *ppr40-2* mutants displayed intermediate survival rates, further supporting the link between ABA hypersensitivity and drought tolerance in these mutants.

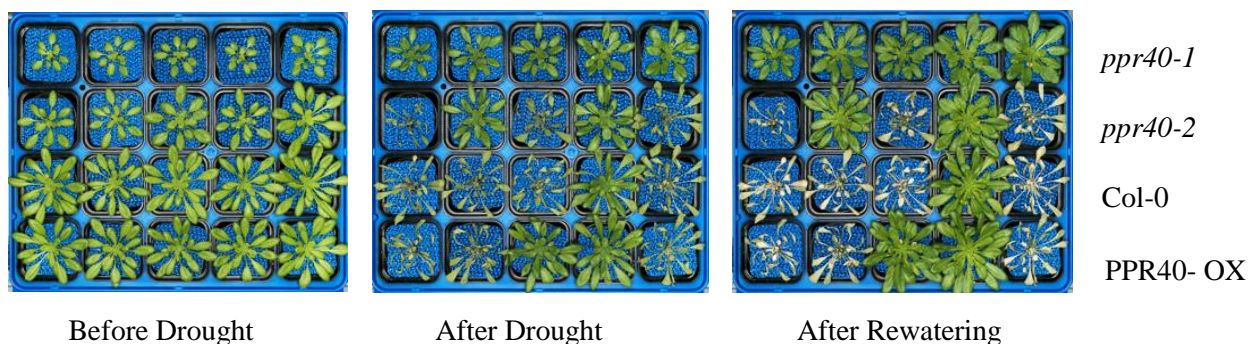


Figure 6: Enhanced drought tolerance in *ppr40-1* and *ppr40-2* mutants compared to Col-0 wild-type plants. Plants cultured in a phenotyping system were subjected to 13 days of water deprivation, followed by re-watering, with representative images at Day 0, after 12 days of water stress, and 6 days post re-watering.

ABA hypersensitivity observed in the *ppr40-1* knockout mutant suggests that *PPR40* might negatively regulate ABA signaling. Conversely, the *ppr40-2* knockdown mutant's intermediate ABA sensitivity points to the leaky nature of that allele. The significant increase in survival rates of the *ppr40-1* mutant under prolonged water stress indicates that its ABA hypersensitivity could confer a certain degree of drought tolerance (Figure 7). Enhanced ABA sensitivity likely contributed to faster stomata closure in the *ppr40-1* mutant, thus reducing water loss through transpiration and maintaining cellular water balance during drought conditions.

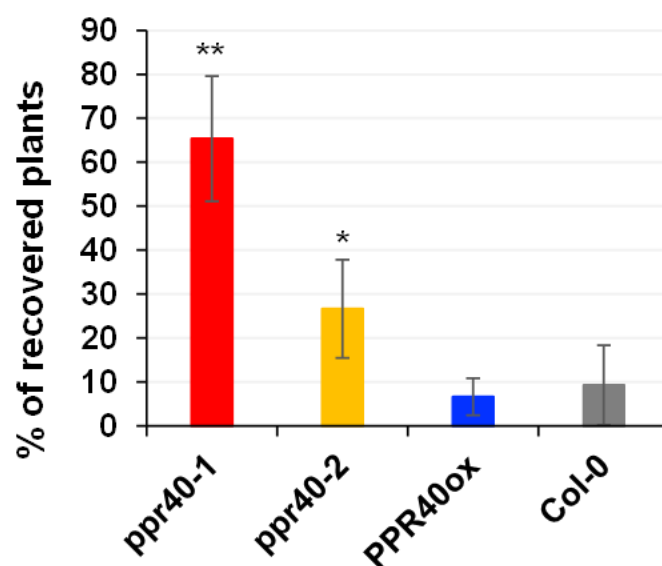


Figure 7: Survival rates in a representative experiment. In this experimental assessment, 80 plants were observed, evaluated in cohorts of 10. The percentage (%) of plants that successfully recovered is presented, with error bars representing standard deviation (n=8). Note that we did not see any significant difference in Col-0 and PPR40-OX lines in survival assay and other physiological experiments that is why we excluded the PPR40 overexpression line from the results. Statistical significance was determined using a T-test, denoting significance with * and ** for p-values less than 0.05 and 0.01, respectively, in comparison to Col-0.

4.2 Confirmation of drought tolerance in *ppr40* mutants through plant phenotyping

To further investigate the drought tolerance of the *ppr40* mutants, we utilized an automatic plant phenotyping platform (PlantScreen™ Compact System, PSI) to compare the growth and morphology of well-watered and water-stressed plants.

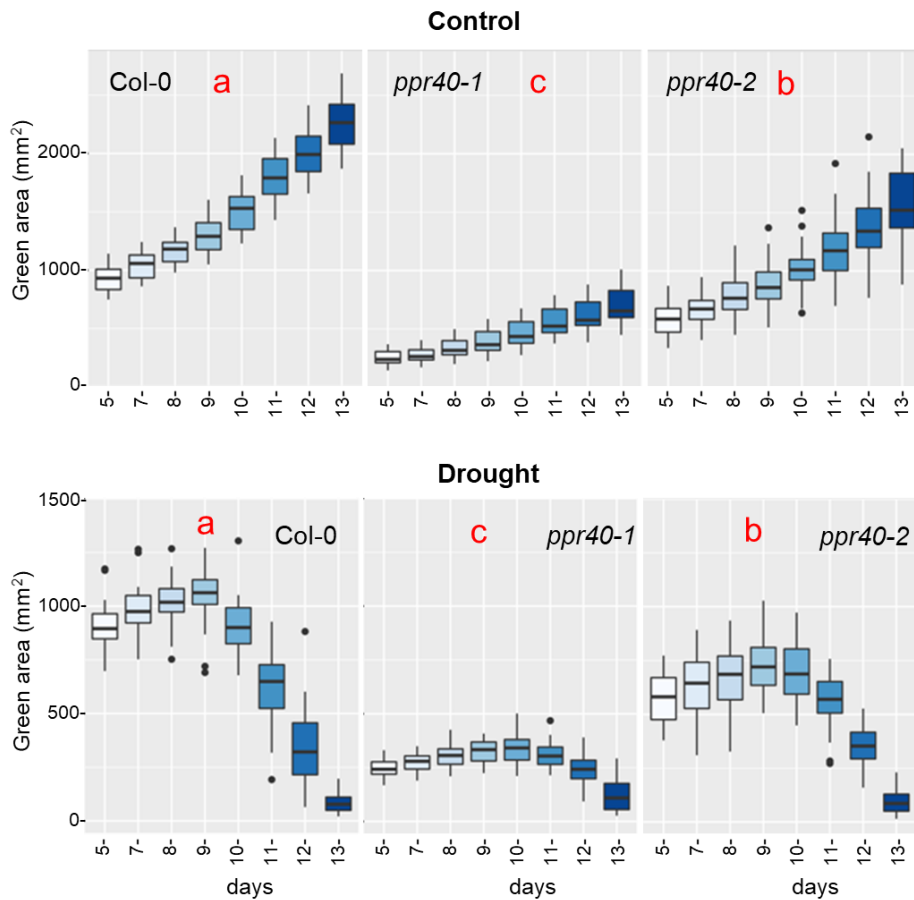


Figure 8: Evaluation of green area through phenotypic analysis. The growth dynamics of *Arabidopsis* plants were assessed through phenotypic analysis, utilizing RGB images captured between 5 and 13 days after watering suspension. Changes in rosette size were quantified by measuring the color-segmented green area of 40 plants for each genotype under two conditions: Control (uninterrupted watering) and Drought (water withdrawal). Statistical comparisons were conducted using the Kruskal-Wallis test for both treatments and genotypes. Different letters (highlighted in red) signify significant differences at $p < 0.05$.

Under normal watering conditions, the growth of rosette sizes in the *ppr40* mutants, namely *ppr40-1* and *ppr40-2*, was significantly reduced compared to the wild-type Col-0 plants. Specifically, *ppr40-1* plants were approximately 70 % smaller, while *ppr40-2* plants were around 30 % smaller than Col-0 plants, confirming the previously reported semi-dwarf phenotype of these mutants (Zsigmond et al., 2008) (Figure 8).

Upon subjecting the plants to water stress, the growth of rosette sizes in all genotypes was severely affected. In the Col-0 plants, the green area continued to grow until day 9 of water deprivation, after which it declined rapidly, indicating a loss of chlorophyll content and deterioration of plant health. However, in the *ppr40* mutants, the decline in the green area

started later, particularly in the *ppr40-1* mutant, which showed the most delayed decline compared to Col-0. The *ppr40-2* mutant exhibited an intermediate response (Figure 8). Normalized parameters for green pixel areas confirmed that the relative rosette sizes of all genotypes grew similarly under water-limited conditions, but the *ppr40* mutants showed better viability compared to Col-0, as their decline in relative green area was delayed (Figure 9).

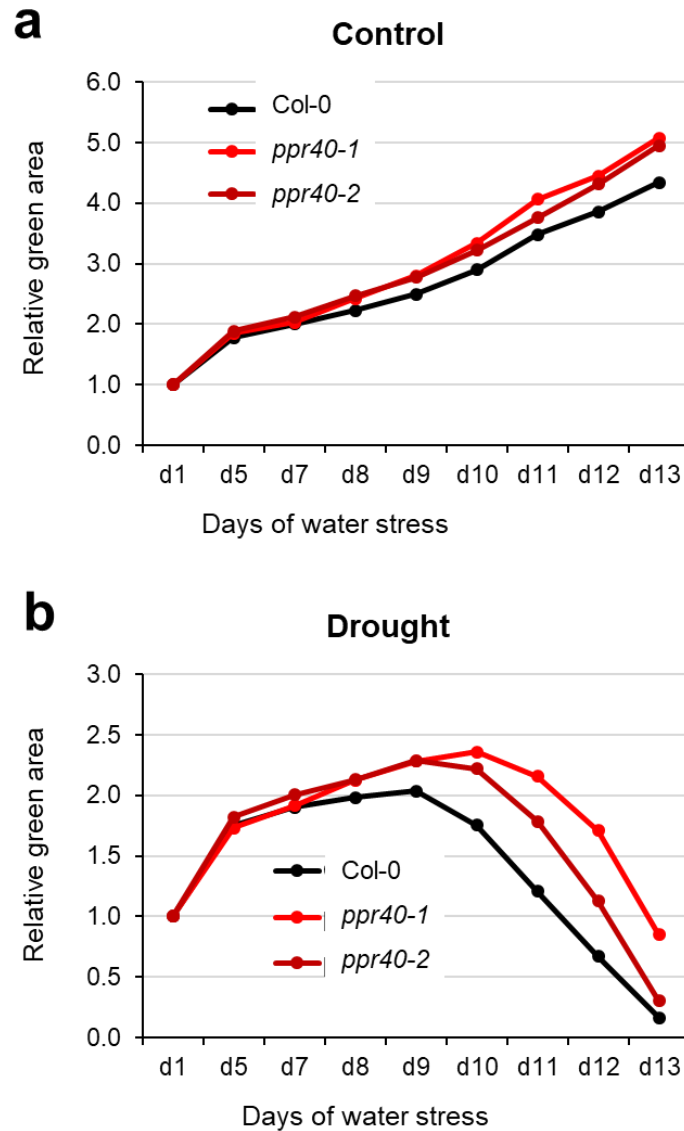


Figure 9: Normalized relative green areas in Col-0, *ppr40-1*, and *ppr40-2* plants detected by plant phenotyping. This figure displays the relative green areas of Col-0, *ppr40-1*, and *ppr40-2* plants as detected through plant phenotyping. The values are presented in a normalized form, relative to the first day of the imaging period, which commenced when watering was suspended (day 1).

To gain further insights into the morphological changes during water stress, we analyzed the hue ratios in well-watered and water-stressed plants. Interestingly, genotype-dependent shifts in hue abundances were observed in plants exposed to 12 days of water deprivation. However, the greenness hue indexes were similar in well-watered plants of all genotypes (Figure 10).

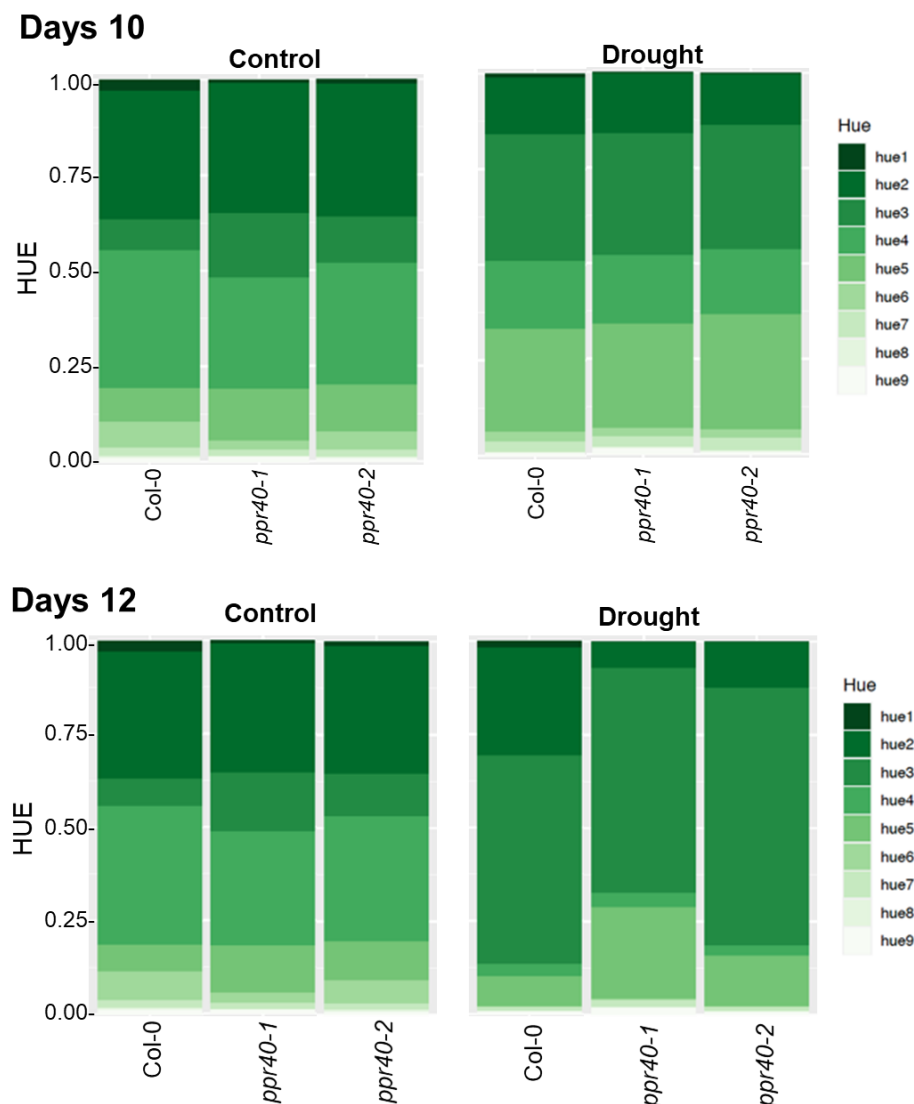


Figure 10: Changes in Greenness Hue Index of Plants After 10 and 12 Days of Drought Detected by RGB Images in the Plant Phenotyping Experiment. This figure illustrates the alterations in the greenness hue index of Col-0, *ppr40-1*, and *ppr40-2* plants following 10 and 12 days of drought, as identified through RGB images in the plant phenotyping experiment. The RGB images were segmented according to the method outlined by Awlia et al. (2016).

RGB images were subsequently used to describe changes in morphological parameters of wild type and mutant plants cultivated in well-watered and water-deprived conditions.

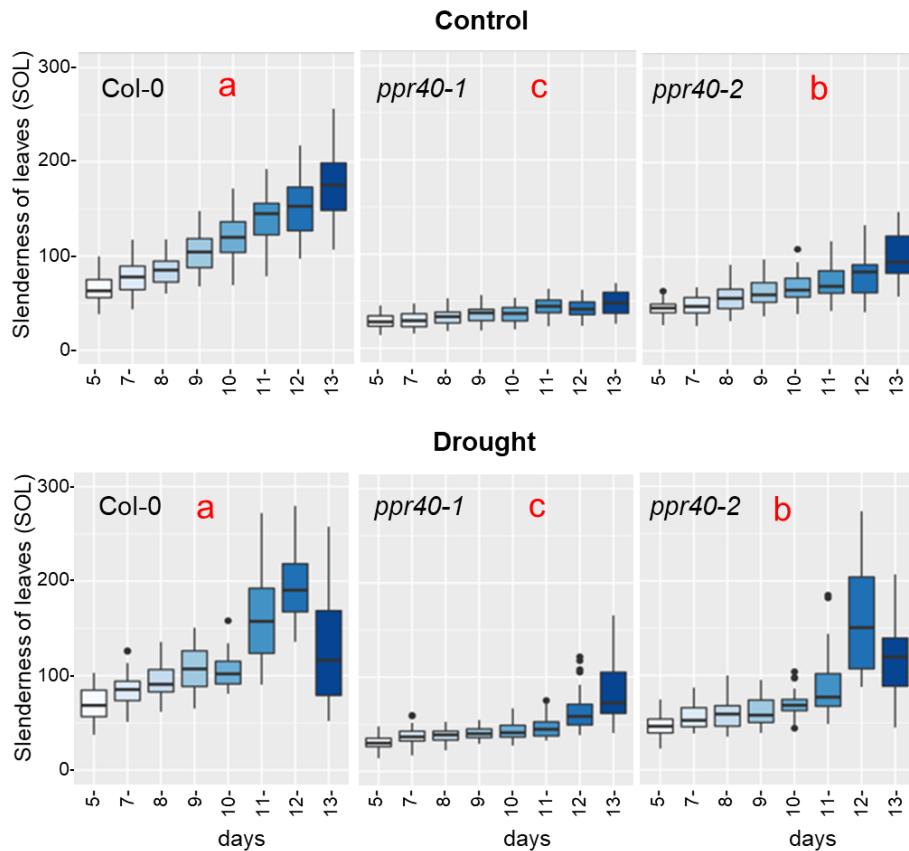


Figure 11: Evaluation of plant morphology through SOL parameter. Plant morphology changes, specifically in terms of leaf slenderness (SOL), were tracked using a phenotyping platform as detailed in Figure 4. SOL values were computed from RGB images under two conditions: Control (uninterrupted watering) and Drought (water withdrawal). Statistical comparisons employed the Kruskal-Wallis test to assess both treatment and genotype effects. Distinct letters (highlighted in red) signify significant differences at $p < 0.05$.

Additionally, we examined the parameter Slenderness of Leaves (SOL), which reflects morphological changes in the rosette growth of well-watered plants. In response to water stress, the SOL values of Col-0 plants became highly variable on day 11 and subsequently dropped rapidly, indicating a significant decline in rosette morphology. In contrast, the *ppr40* mutants showed a slower change in SOL values, suggesting better preservation of plant morphology during drought stress, especially in the *ppr40-1* mutant (Figure 11).

We also investigated the compactness of leaves as an indicator of rosette growth morphology in response to water stress. Like the patterns observed with SOL, the compactness values exhibited noteworthy changes under drought conditions. For Col-0 plants, the compactness

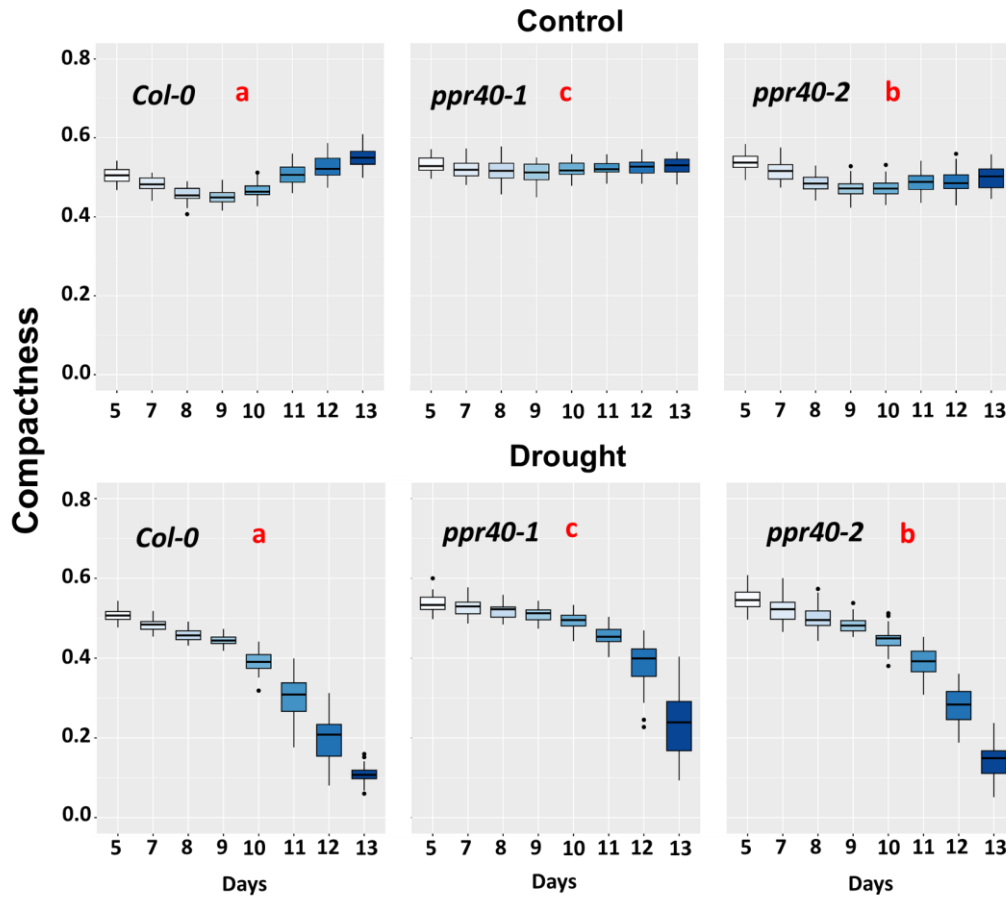


Figure 12: Assessment of plant compactness. Changes in plant morphology, particularly in compactness, were monitored utilizing a phenotyping platform. The values were derived from RGB images under two conditions: Control (continuous watering) and Drought (water deprivation). Statistical analysis was conducted using the Kruskal-Wallis test to evaluate treatment and genotype impacts. Different letters (highlighted in red) indicate significant variations at $p < 0.05$.

values displayed increased variability around day 11, followed by a rapid decline, indicative of a significant alteration in rosette morphology due to water stress (Figure 12). Conversely, the *ppr40* mutants, particularly the *ppr40-1* mutant, demonstrated a more gradual shift in compactness values, suggesting a more resilient response to drought stress and better preservation of rosette morphology. This alignment in results between SOL and compactness further underscores the adaptive advantages conferred by the *ppr40* mutants under water stress conditions.

Overall, our plant phenotyping data provided compelling evidence that the *ppr40* mutants exhibit enhanced drought tolerance compared to the wild-type Col-0 plants. The delayed decline in rosette size, sustained greenness, and better-preserved morphology in the *ppr40* mutants under water-limited conditions indicate their improved ability to withstand drought stress, further supporting the link between ABA hypersensitivity and drought tolerance in these mutants.

4.3 Confirmation of drought tolerance in *ppr40* mutants through physiological parameters

Physiological parameters were employed to further investigate the drought tolerance of the *ppr40* mutants. Enhanced ABA sensitivity in these mutants could potentially lead to faster stomata closure, helping the plants preserve water during periods of water shortage. To assess the water status of stressed plants, we determined the relative water content (RWC) in fully hydrated and dehydrated wild-type Col-0 plants and the *ppr40* mutants.

Under normal watering conditions, RWC was similar among all tested genotypes. However, under water stress, Col-0 plants experienced a substantial 75 % reduction in RWC, indicating a severe water deficit. In contrast, the *ppr40-1* mutant exhibited a more efficient water retention mechanism, with only a 40 % reduction in RWC, while the *ppr40-2* mutant showed an intermediate response with a 63 % reduction (Figure 13). These findings suggest that the water-stressed *ppr40-1* mutant retained more water compared to Col-0, which correlated with slower wilting and higher viability observed in these mutants.

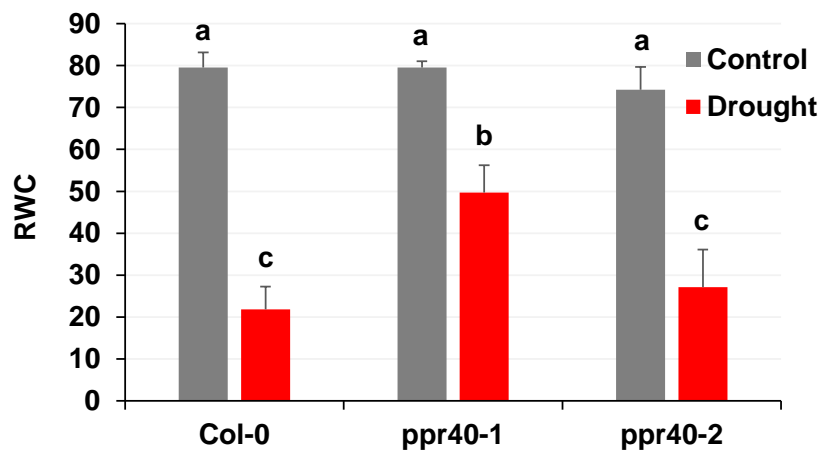


Figure 13: RWC in response to water deprivation. Arabidopsis *ppr40-1* and *ppr40-2* mutants, along with Col-0 wild-type plants, were subjected to 10 days of water deprivation to assess RWC. The experiments, performed in a growth chamber, were repeated three times. Error bars indicate standard deviation. Statistical analysis involved Two-way ANOVA followed by the Tukey test. Different letters signify significant differences at $p < 0.05$.

Proline accumulation is a well-known physiological response to water deprivation in higher plants and is associated with osmotic and oxidative stress defenses (Alvarez et al. 2022). In standard growth conditions, the *ppr40* mutants, particularly *ppr40-1*, exhibited two to four times higher proline content than wild-type plants (Figure 14). In response to drought stress, proline levels gradually increased in Col-0 plants after 7 days of water deprivation. In contrast, the *ppr40-1* mutant showed little change in proline levels until day 8 of water stress, after which it started to increase. The *ppr40-2* mutant displayed slower kinetics of proline accumulation compared to Col-0 but faster than the *ppr40-1* mutant, aligning with its intermediate phenotype (Figure 14).

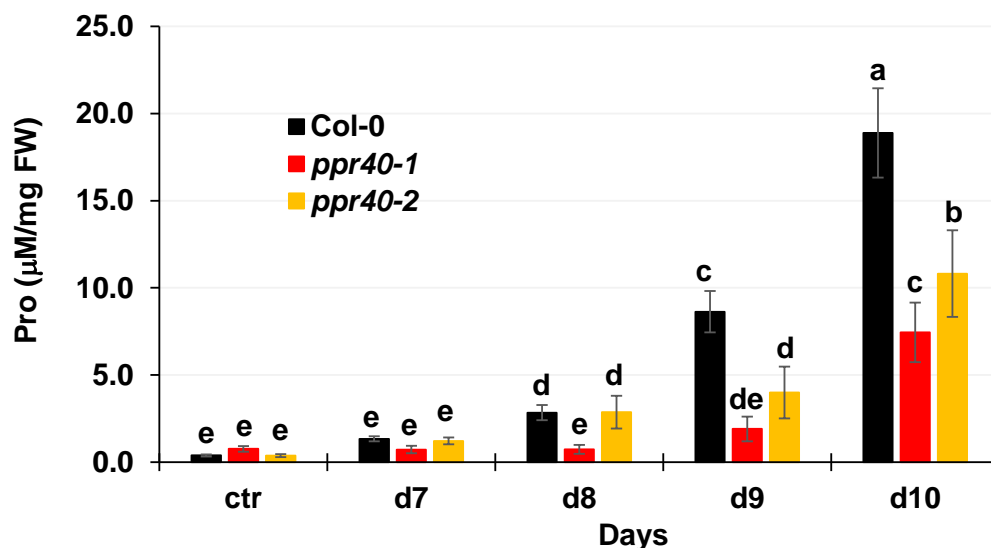


Figure 14: Proline accumulation in response to water deprivation. The alteration in proline content was examined in wild type (Col-0) and mutant (*ppr40-1*, *ppr40-2*) plants subjected to water withdrawal for up to 10 days. The experiments were conducted in a growth chamber, and proline levels were assessed as a response to the stress. Statistical analysis utilized Two-way ANOVA, Fisher’s LSD, and Tukey test. Distinct letters represent significant differences at $p < 0.05$.

Proline metabolism is regulated by two key enzymes, the Δ -Pyrroline Carboxylate Synthase (P5CS) and the Proline Dehydrogenase (PDH), which control the first steps of proline biosynthesis and catabolism, respectively (Szabados and Saviouré 2010). In Arabidopsis, these enzymes are encoded by two genes with distinct transcriptional regulations. *P5CS1* is an ABA-regulated gene essential for stress-dependent proline accumulation (Székely et al., 2008). We found that *P5CS1* expression was enhanced sevenfold in drought-stressed wild-type plants,

while three to fivefold enhancements were detected in the *ppr40-1* and *ppr40-2* mutants, respectively (figure 15). In contrast, the expression of the *PDH1* gene remained unchanged in all conditions and was similar in wild-type and mutant plants (Figure 15). These results indicate that the less efficient activation of *P5CS1*, responsible for proline biosynthesis, contributes to the reduced proline accumulation in the *ppr40* mutants under water-limited conditions.

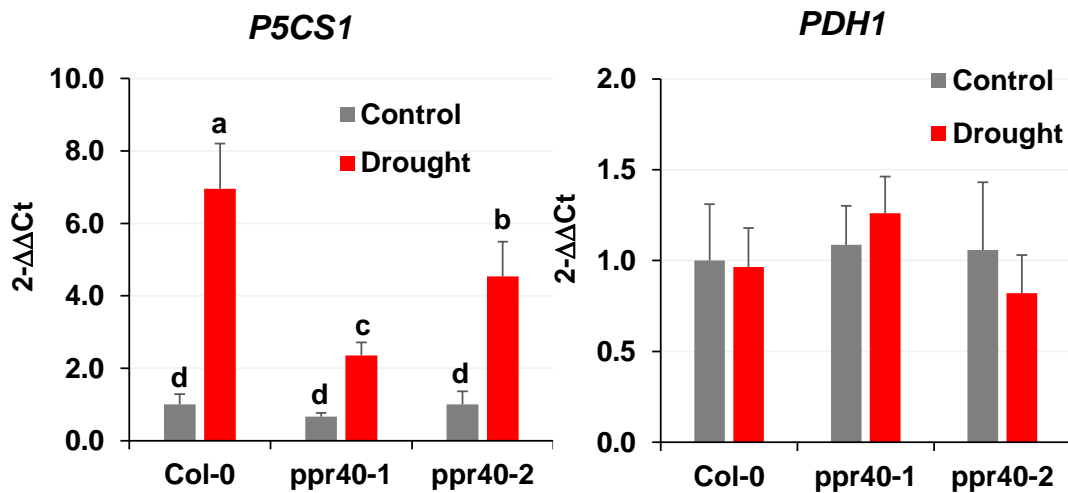


Figure 15: Expression of *P5CS1* and *PDH1* genes in water-stressed plants. The expression patterns of *P5CS1* and *PDH1* genes were investigated in response to water deprivation in *ppr40-1*, *ppr40-2* mutants, and wild-type (Col-0) plants. The experiments carried out in a growth chamber, involved both water-stressed and well-watered plants after 8 days of treatment. Relative expression is presented, where 1 corresponds to transcript levels in non-treated Col-0 plants. Statistical analysis employed Two-way ANOVA, Fisher’s LSD, and Tukey test. Different letters denote significant differences at $p < 0.05$.

Taken together, these physiological parameters provide compelling evidence that the *ppr40* mutants exhibit enhanced drought tolerance compared to the wild-type Col-0 plants. The superior water retention and slower wilting in the *ppr40* mutants, as well as the altered kinetics of proline accumulation and *P5CS1* expression, highlight the involvement of *PPR40* in regulating plant responses to water stress. These findings further support the notion that ABA hypersensitivity of the *ppr40* mutants can confer drought tolerance and underscore the potential of *PPR40* as a promising target for improving drought resilience in crops.

4.4 Stomatal conductance patterns in *ppr40-1* mutant highlight ABA hypersensitivity and altered responses to water stress

Stomatal conductance, a key indicator of gas exchange and transpiration, is intricately linked to stomatal aperture. The ABA hypersensitivity observed in the *ppr40-1* mutant was associated with accelerated stomatal closure. To unravel the implications of the *ppr40-1* mutation on stomatal conductance, a comparative analysis was performed between water-stressed wild-type and mutant plants.

In well-watered conditions and up to three days after withholding water, stomatal conductance in the *ppr40-1* mutant was consistently lower than in Col-0. The rate of decline in stomatal conductance of Col-0 plants was more rapid than of *ppr40-1* mutant under water-restricted conditions. Under severe water deprivation, stomatal conductance became significantly reduced in both genotypes (Figure 16).

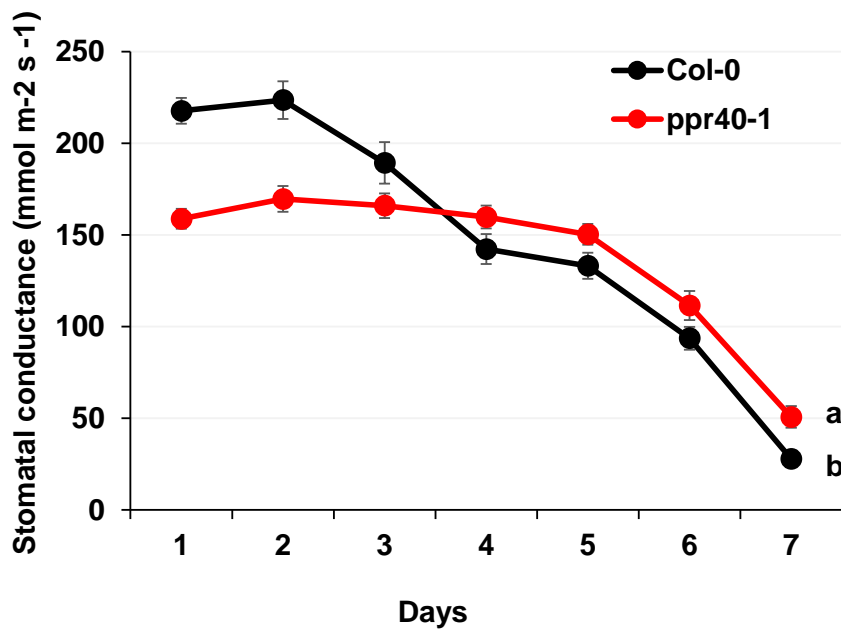


Figure 16: Impact of water deprivation on stomatal conductance. The effect of water deprivation on stomatal conductance in Col-0 wild-type and *ppr40-1* mutant plants is illustrated. Four-week-old plants underwent a 7-day water deprivation, with stomatal conductance measured at daily intervals. Error bars represent standard deviation. The experiments, conducted in a growth chamber, were replicated three times. Statistical analysis employed Two-way ANOVA followed by Tukey test. Distinct letters indicate significant differences at $p < 0.05$.

4.5 Insights from a metabolomics survey under water stress conditions

Plant mitochondria, recognized for their vital roles in energy supply and redox control, function as central metabolic hubs influencing diverse metabolic pathways through respiration (Millar

et al. 2011b). To unravel the repercussions of the *ppr40-1* mutation on mitochondrial metabolism, we conducted a targeted metabolomics survey with a focus on the tricarboxylic acid (TCA) cycle, sugar, and amino acid metabolic pathways.

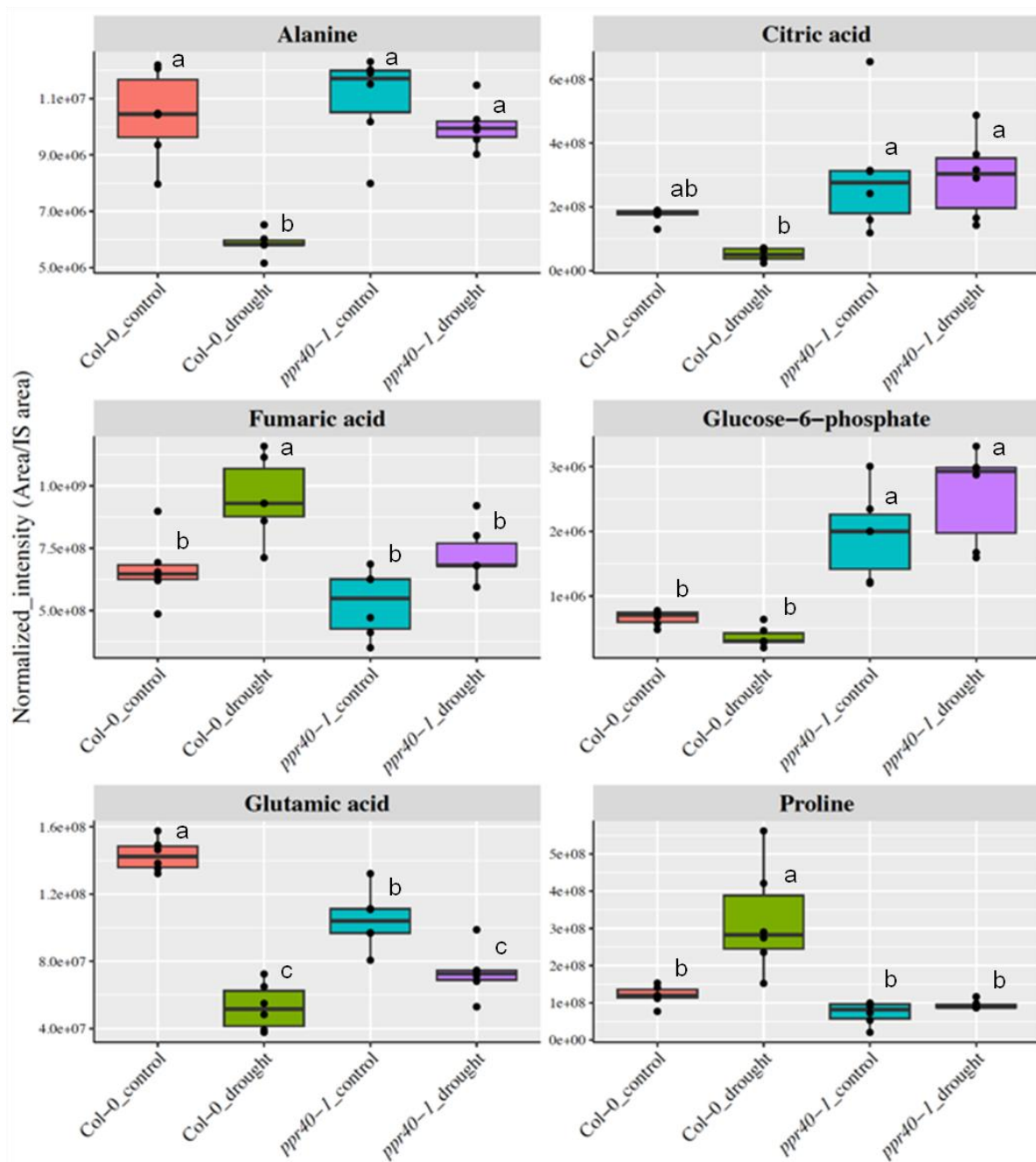


Figure 17: Metabolic profiles of selected metabolites in Col-0 wild-Type and *ppr40-1* Mutant Plants. The metabolic profiles of six chosen metabolites were assessed in leaves of 4-week-old Col-0 wild-type and *ppr40-1* mutant plants. The analysis was conducted using LC/MS under both well-watered (control) and water-restricted (drought) conditions.

Under conditions of water deprivation, significant alterations in the concentrations of various organic acids within the TCA cycle and amino acids were observed, with distinctive responses in the *ppr40-1* mutant (Figure 17). Drought-induced reductions in alanine and glutamate content in Col-0 plants were only moderately abated in the *ppr40-1* mutant. Notably, drought-dependent proline accumulation was lower in the *ppr40-1* mutant compared to wild-type plants.

The metabolomics survey also revealed differences in citric acid and glucose-6-phosphate concentrations between wild-type and *ppr40-1* plants under water stress. While concentrations of these metabolites decreased in response to water stress in Col-0 plants, they were elevated in the *ppr40-1* mutant, regardless of water availability. Additionally, fumaric acid content was lower in *ppr40-1* than in wild-type plants, and only a moderate enhancement was observed under drought conditions in the mutant.

These findings emphasize the significant impact of the *ppr40-1* mutation on various metabolic pathways, including the mitochondrial TCA cycle. The observed alterations in metabolite profiles provide valuable insights into the intricate metabolic responses associated with the *ppr40-1* mutation, shedding light on the broader metabolic consequences in the context of water stress conditions.

4.6 Enhanced stability of photosynthesis in drought-stressed *ppr40* mutants

Photosynthesis is a critical physiological process that is highly sensitive to drought stress in plants. To investigate the changes in photosynthesis in the *ppr40* mutants under water stress, we monitored chlorophyll fluorescence through phenotyping image analysis in plants grown under standard and water-deprived conditions.

Under normal watering conditions, the maximum quantum yield of PSII photochemistry (Fv/Fm) was similar among wild-type and mutant plants, showing values of 0.83-0.84 during the observation period. However, when watering was suspended, Fv/Fm values in the wild-type Col-0 plants remained relatively stable until the 10th day of water deprivation, after which they sharply dropped, reaching an average of 0.57 on day 13. In contrast, the *ppr40-1* mutant exhibited a more stable Fv/Fm value under such conditions, with a slower decline that started on the 12th day after watering was stopped. On day 13, the average Fv/Fm value of *ppr40-1* was still around 0.77. The *ppr40-2* mutant showed an intermediate response, with a faster decline in Fv/Fm compared to *ppr40-1* but still more stable than Col-0 (Figure 18) The image-based analysis of chlorophyll fluorescence over time revealed significant differences between

the wild-type and *ppr40* mutant plants in the maximum quantum yield of PSII, a widely used photosynthetic parameter in plant stress biology. These differences indicated that the photosynthetic electron transport remained functional for more extended periods in the drought-stressed *ppr40* mutants than in wild-type plants.

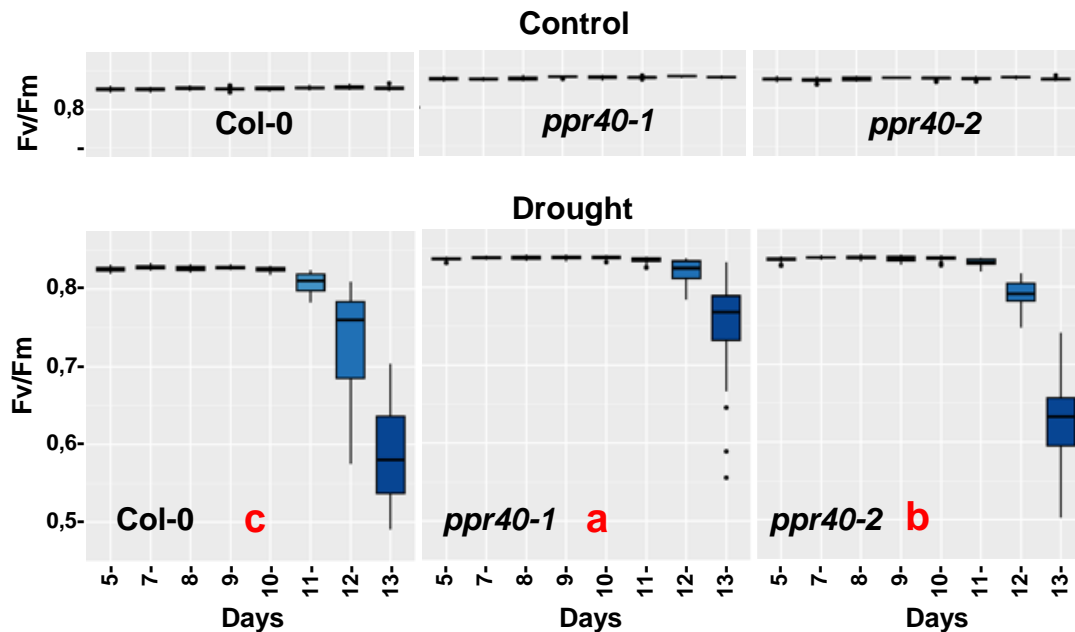


Figure 18: Impact of water deprivation on photosynthetic parameters in Col-0 wildtype and *ppr40* Mutant Plants. This figure depicts the influence of water deprivation on photosynthetic parameters in Col-0 wild-type and *ppr40* mutant plants. Chlorophyll fluorescence (ChlF) imaging was employed to monitor alterations in photosynthetic parameters between water-stressed and well-watered plants, utilizing an automated plant phenotyping platform. The change in the Fv/Fm parameters is presented as an average from 40 plants. Control conditions involved uninterrupted watering, while drought conditions entailed water withdrawal. Statistical analysis employed the Kruskal-Wallis test to compare treatments and genotypes, with different letters (highlighted in red) denoting significant differences at $p < 0.05$.

To gain further insights into the photosynthetic efficiency in drought-stressed plants, we analyzed electron transport rates (ETR) in separate experiments using plants cultured under well-watered and water-deprived conditions in growth chambers. Under standard conditions, ETR(II) values were similar in wild-type and *ppr40* mutants. However, when subjected to 10 days of water deprivation, ETR(II) in the Col-0 wild-type plants was reduced by 50 %.

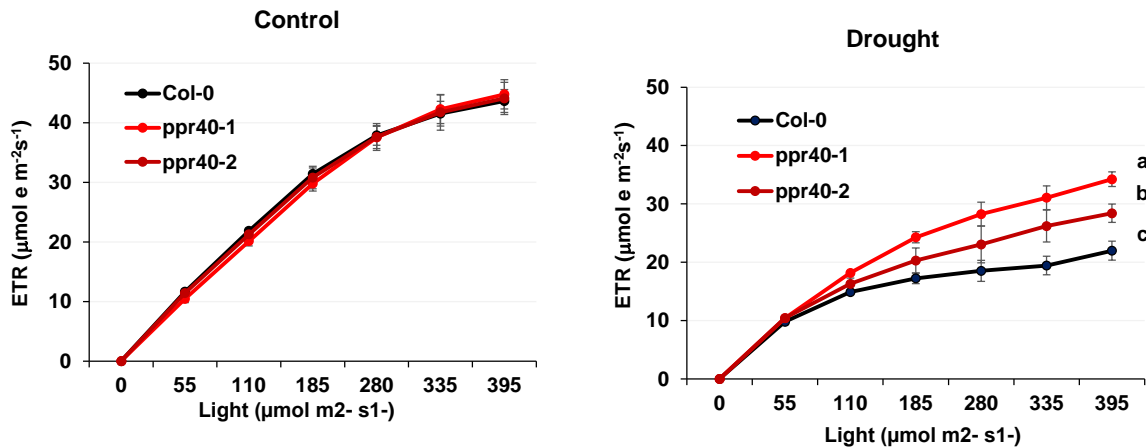


Figure 19: Quantitative analysis of ETR. This figure presents a quantitative examination of electron transport rates in *ppr40-1* and *ppr40-2* mutants, as well as in wild-type (Col-0) plants. ETR(II) was measured in dark-adapted conditions using a pulse-amplitude-modulated chlorophyll fluorometer (Maxi-PAM). The ETR values were derived from both well-watered (Control) and water-stressed plants subjected to 10 days of water deprivation (Drought). Error bars represent standard deviation (n=3), and the experiments were independently repeated three times. Statistical analysis involved Two-way ANOVA and Tukey test. Different letters indicate significant differences at $p < 0.05$.

Remarkably, this reduction in ETR(II) was significantly alleviated in the *ppr40-1* mutant, which exhibited a 35 % higher ETR(II) compared to the drought-stressed Col-0 plants. The ETR(II) values in the *ppr40-2* mutant were intermediate between Col-0 and *ppr40-1* under water-stressed conditions (Figure 19). These results provide strong evidence that photosynthesis is less affected by water stress in the *ppr40* mutants compared to wild-type *Arabidopsis* plants.

The observed differences in the maximum quantum yield of PSII and ETR(II) further supported the notion that photosynthesis is more stable in the drought-stressed *ppr40* mutants. The correlation between the phenotypic changes, other physiological data, and the photosynthetic responses in the knockout and knock-down mutants underscores the role of PPR40 in enhancing drought tolerance.

4.7 Oxidative damage is alleviated by *ppr40* mutations

ROS generation is a common response to environmental stress in plants. Photosynthesis is a major source of superoxide, which is rapidly converted to hydrogen peroxide in stressed plants. Increased levels of ROS may induce oxidative stress, causing peroxidation of different macromolecules and lipids (Møller et al. 2007). The photosynthetic parameters of wild-type and mutant plants were affected differently by drought. Therefore, we wanted to investigate oxidative damage during water stress.

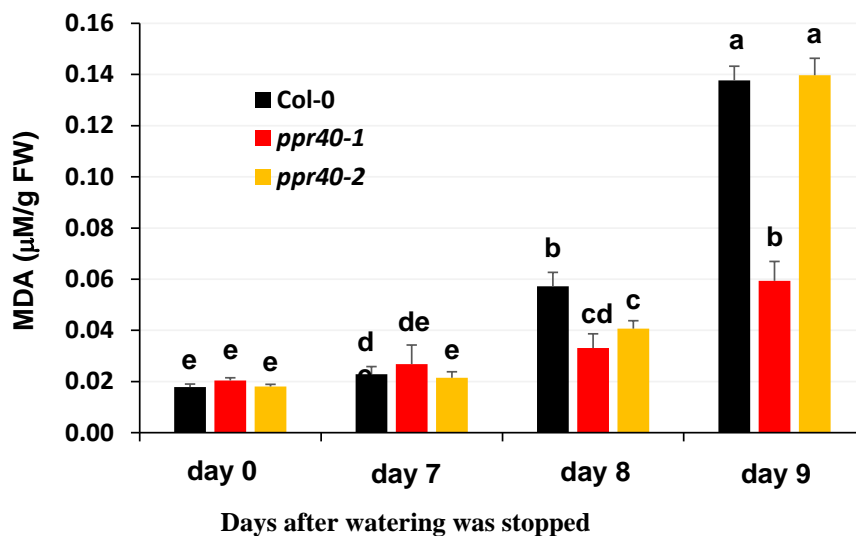


Figure 20: Lipid peroxidation rates in response to water deprivation. This figure illustrates the lipid peroxidation rates in Col-0 wild-type and *ppr40* mutant plants under both well-watered and water-stressed conditions. The plants were cultured in growth chambers under standard conditions for 4 weeks, followed by a 10-day water withdrawal. MDA levels, indicative of oxidative damage, are presented in response to gradual stress. Statistical analysis involved Two-way ANOVA and Tukey test. Different letters signify significant differences at $p < 0.05$.

To assess lipid peroxidation, we measured malondialdehyde (MDA) levels, which serve as an indicator of oxidative damage. As expected, MDA levels increased over time in response to drought stress, indicating enhanced lipid peroxidation and oxidative damage. The increase in lipid peroxidation became evident after the 7th day of water deprivation. Subsequently, MDA accumulated more rapidly and reached 2 to 2.5 times higher levels in the wild-type Col-0 plants compared to the *ppr40-1* mutant. The *ppr40-2* mutant displayed a slower increase in lipid peroxidation compared to the wild type, but it eventually reached a level comparable to Col-0 after nine days of water deprivation (Figure 20). These findings suggest that the drought-dependent oxidative damage was significantly lower in the *ppr40-1* mutant compared to both *ppr40-2* and wild-type plants.

ROS signals and ABA signals are known to interact and modulate stress responses, including the activation of stress-induced genes (Mittler and Blumwald 2015). The differences observed in lipid peroxidation rates led us to investigate whether ROS-induced gene expression might be altered in the *ppr40* mutants.

We focused on *ZAT12*, a well-known transcription factor responsible for regulating the expression of numerous ROS-induced genes (Davletova et al. 2005). Upon drought treatment, transcript levels of *ZAT12* were enhanced in all genotypes, but the induction was notably lower in the *ppr40* mutants, especially in the *ppr40-1* mutant (Figure 21). This result suggests that the activation of ROS-dependent gene expression is attenuated in the *ppr40* mutants.

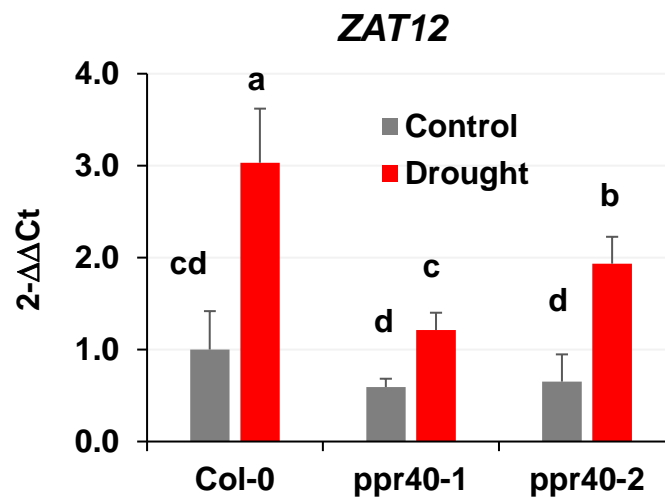


Figure 21: Expression of ROS-induced *ZAT12* gene in drought-stressed plants. This figure depicts the expression patterns of the ROS-induced *ZAT12* gene in plants subjected to drought stress for 8 days. The relative transcript levels are presented, where 1 corresponds to values measured in Col-0 plants under control conditions. The reference genes *Actin2* and *UBC18* were used for normalization. Averages of three replicates are shown, with standard deviation indicated by the bars on the diagrams. Statistical analysis utilized Two-way ANOVA and Tukey test. Different letters indicate significant differences at $p < 0.05$.

These results indicate that the *ppr40* mutants display reduced oxidative damage under water stress, as evidenced by lower lipid peroxidation rates compared to wild-type Col-0 plants. Moreover, the attenuated induction of the ROS-responsive transcription factor, *ZAT12*, in the *ppr40* mutants further supports the notion of altered ROS signaling.

4.8 Modulation of drought-induced gene expression by *PPR40*.

Water deprivation induces significant changes in the gene expression profiles of plants, with hundreds of genes being either upregulated or downregulated under drought conditions. A key player in the stress response is ABA, the primary stress hormone, which not only promotes rapid physiological responses, such as stomata closure during high osmotic conditions but also induces the expression of a large set of dehydration-responsive genes (Finkelstein 2013).

To investigate the potential effect of the *ppr40* mutation on ABA-induced transcriptional regulation, we monitored the transcript levels of selected target genes from 7 days drought-stressed plants. *RAB18*, an ABA-induced dehydrin gene, showed a 30 to 40 times increase in expression in response to water stress in wild-type plants. However, the transcript levels of *RAB18* were around 80 % lower in the drought-stressed *ppr40-1* mutant, and *ppr40-2* exhibited approximately half the expression level observed in Col-0 plants. Another drought-responsive gene, *RD29A*, which is regulated by both ABA-dependent and independent signals, was induced in water-stressed plants, although the difference between wild-type and mutant plants was not as pronounced as in the case of *RAB18* (Figure 22a).

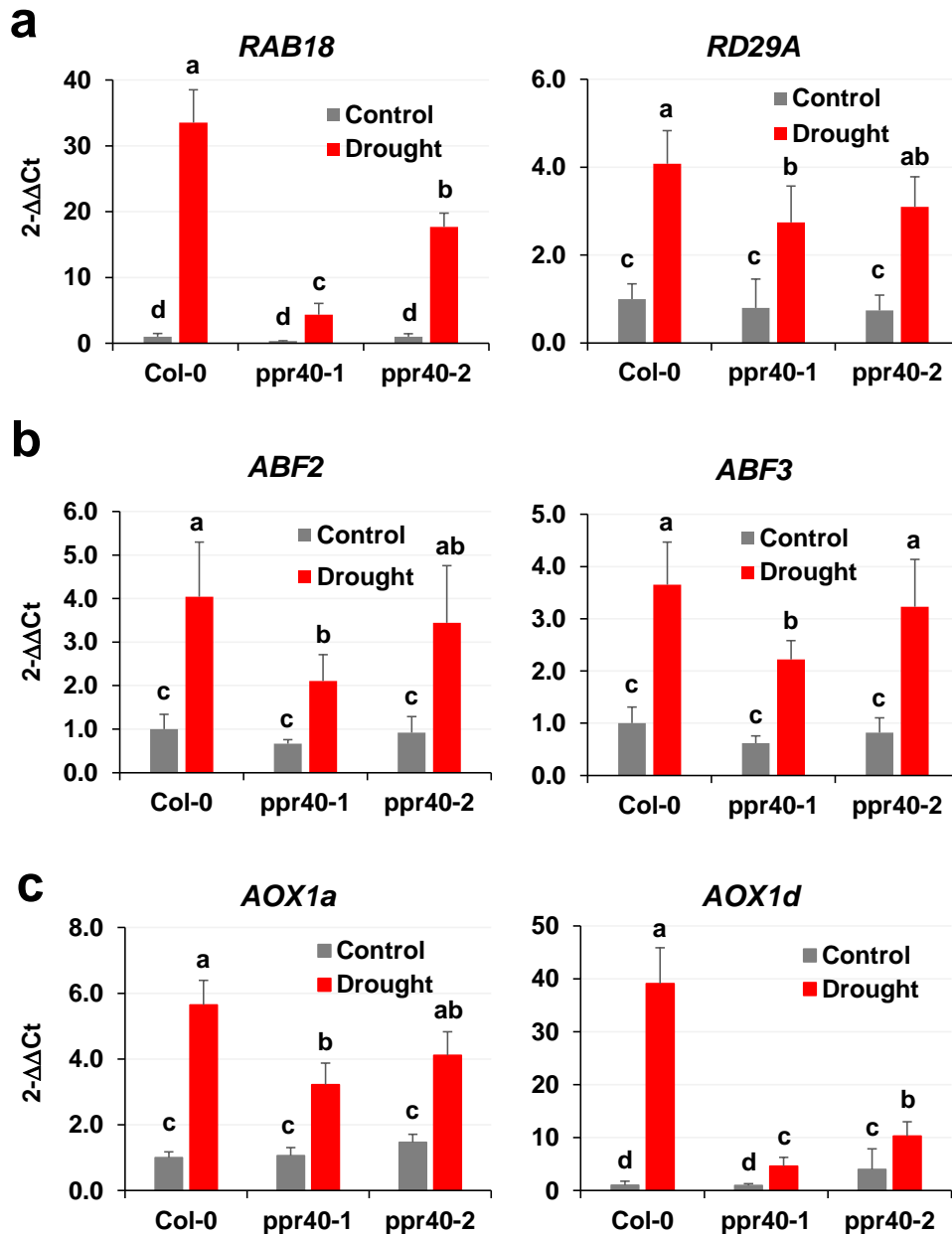


Figure 22: Expression profiles of selected stress-induced genes in response to water availability. This figure illustrates the expression patterns of stress-induced genes under water-limited and well-watered conditions. Transcript levels of a) *RD29A* and *RAB18*, b) *ABF2* and *ABF3*, and c) *AOX1a* and *AOX1d* genes were quantified using qRT-PCR, with *Actin2* and *UBC18* serving as reference genes for normalization. Relative expression levels are presented, where a value of 1 corresponds to transcript levels in Col-0 control plants. The data represents the average of three replicates, with standard deviation indicated by the bars on the diagrams. Statistical analysis involved Two-way ANOVA and Tukey test, with different letters denoting significant differences at $p < 0.05$.

We also examined the expression levels of bZIP-type *ABF* transcription factors, which are key regulators of ABA-induced transcription. *ABFs* bind to ABA-responsive cis promoter elements

(ABRE motifs) and play a central role in ABA signaling (Finkelstein 2013). Under well-watered conditions, the expression of *ABF2* and *ABF3* was similar in wild-type plants and mutants. However, in response to water stress, the transcript levels of *ABF2* and *ABF3* increased three to four times in Col-0 plants and approximately twice in the *ppr40-1* mutant. The induction of these *ABF* genes in the *ppr40-2* mutant was intermediate between Col-0 and *ppr40-1* (Figure 22b).

Furthermore, we examined the expression of two stress-responsive alternative oxidases (AOX) genes, *AOX1a* and *AOX1d*, which function as non-energy conserving terminal oxidases in the mitochondrial electron transport and can alleviate over-reduction of the mitochondrial electron transport chain (mETC) during stress (Clifton et al. 2006). *AOX* genes responded to water stress in wild-type plants, but their activation was less efficient in the *ppr40* mutants compared to wild-type. Particularly, *AOX1d* expression, a dominant stress-induced *AOX* gene, showed a notable difference in expression levels between wild-type and mutant plants (Figure 22c).

These results collectively suggest that drought-responsive transcriptional activation is less efficient in the *ppr40* mutants, especially in *ppr40-1*. This difference is likely a consequence of the hydration status, as indicated by the RWC data. The reduced water loss in the *ppr40-1* mutant mitigated dehydration and resulted in moderate osmotic stress, lower ROS accumulation, and reduced oxidative stress, leading to minor stress-responsive gene activation. In conclusion, the findings highlight the role of PPR40 in modulating drought-induced gene expression, particularly under severe water stress conditions. The altered expression of stress-responsive genes, such as *RAB18*, *RD29A*, *ABFs*, and *AOX*, in the *ppr40* mutants provides valuable insights into the molecular mechanisms underlying the enhanced drought tolerance observed in these mutants.

4.9 Hormone signaling modulation under drought stress

Response to water depletion is regulated by various hormones in higher plants. In investigating the potential impact of *ppr40* mutations on hormone signaling, we scrutinized transcript levels of several hormone-regulated genes in *ppr40-1* and *ppr40-2* mutants compared to the wild-type Col-0 under standard and water-restricted conditions (Figure 23). Notably, the genes *LAX3* and *AUX1*, integral to auxin signal transduction (Péret et al. 2012), exhibited downregulation in response to water deprivation in wild-type plants, a phenomenon less pronounced or absent in the *ppr40* mutants.

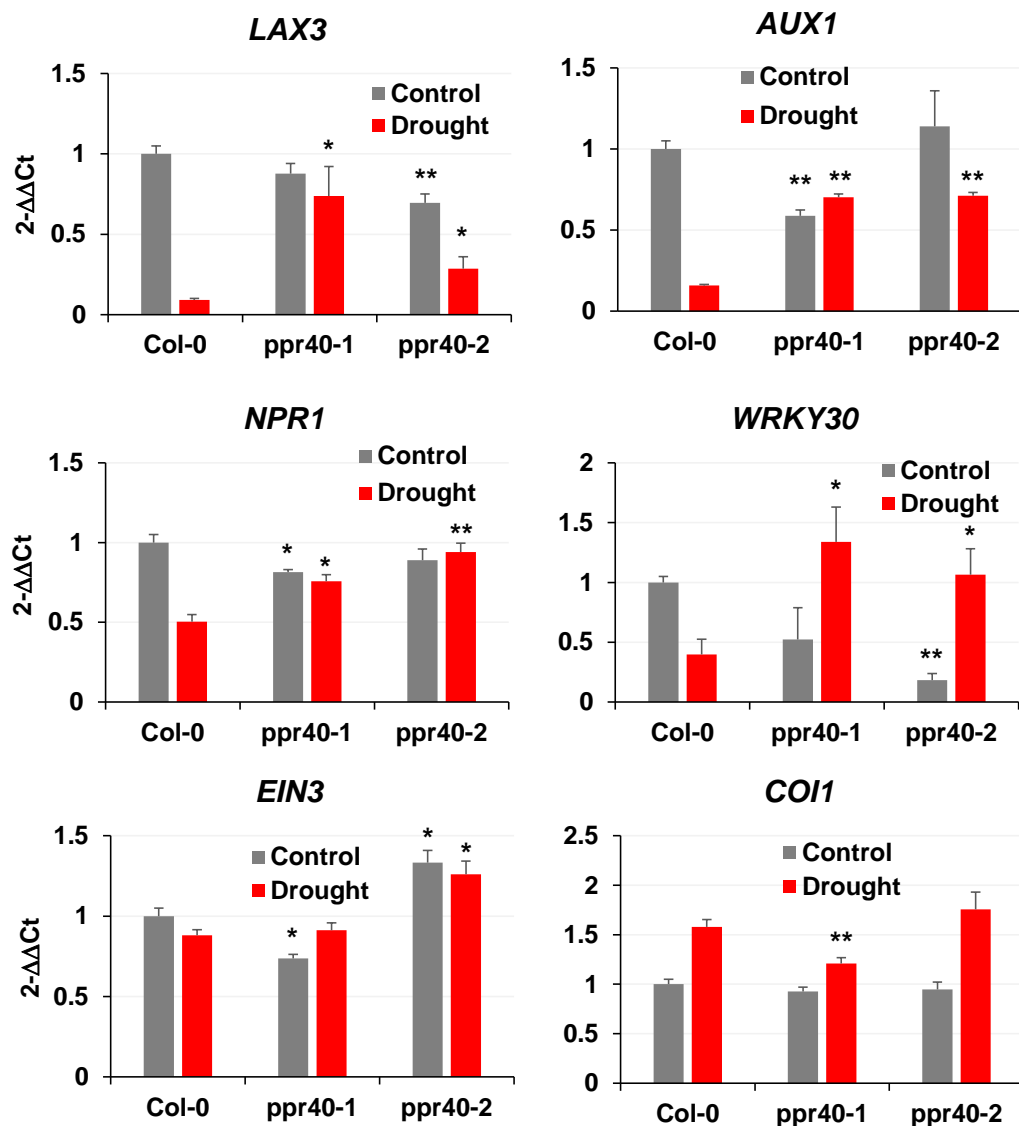


Figure 23: Expression profiles of hormone-regulated genes in Col-0 wild type, *ppr40-1*, and *ppr40-2* mutant plants under water stress. This figure presents the expression profiles of hormone-regulated genes *LAX3*, *AUX1*, *NPR1*, *WRKY30*, *EIN3*, and *COI1*, in Col-0 wild-type, *ppr40-1*, and *ppr40-2* mutant plants subjected to water stress. Relative expression levels are depicted, where 1 corresponds to the transcript levels of Col-0 in control plants. The data represents the average of three replicates, with standard deviation indicated by the bars on the diagrams. Statistical analysis involved Two-way ANOVA and Tukey test, with different letters denoting significant differences at $p < 0.05$.

Examining the salicylic acid (SA) signaling pathway, we focused on *NONEXPRESSOR OF PATHOGENESIS-RELATED GENES1 (NPR1)*, a pivotal regulator in pathogen response pathways (Chen et al. 2021a). While water stress halved *NPR1* expression in Col-0 plants, this

reduction was not observed in the *ppr40* mutants, suggesting a distinct regulatory role for PPR40 in SA signaling under stress conditions.

Considering the environmental responsiveness of the *WRKY30* transcription factor, which integrates signals from various stimuli and hormones (Jiang et al. 2017; András et al. 2019), we observed a reduction in *WRKY30* transcript levels in drought-treated wild-type plants. Intriguingly, drought-dependent enhancement in *WRKY30* expression was observed in *ppr40* mutants in contrast to Col-0 plants, where water deprivation reduced *WRKY30* transcription (Figure 23).

Turning our attention to ethylene signaling, the key transcriptional regulator *EIN3* (Song et al. 2022) displayed minor alterations under drought conditions, with only marginal differences detected in the *ppr40* mutants. Conversely, the jasmonate receptor complex component *COII*, essential in wound and jasmonate-dependent signaling (Wasternack and Song 2017), exhibited moderate upregulation in response to water stress. Interestingly, the *ppr40-2* and *ppr40-1* mutants displayed either no or only slight differences in *COII* transcript levels, suggesting a potential role for *PPR40* in modulating jasmonate-dependent signaling pathways.

Our transcript analysis implies that *PPR40* not only influences ABA-dependent regulation but also has a regulatory impact on pathways controlled by other hormones, such as auxin, salicylic acid, and brassinosteroids. These findings contribute to a comprehensive understanding of the multifaceted role of *PPR40* in hormone signaling pathways, shedding light on its intricate regulatory network under stress conditions.

5. Discussion

The findings presented in this thesis have shed light on the role of the mitochondria localized PPR40 protein in enhancing drought tolerance in Arabidopsis plants. Earlier data demonstrated that PPR40 directly influences cellular respiration and is involved in responses to salt, osmotic, and oxidative stresses (Zsigmond et al. 2008). While most PPR proteins are known to bind RNA and participate in post-transcriptional processing of organelle-encoded RNA sequences, PPR40 stands out as an exception. It does not bind RNA nor engage in RNA processing, yet it exerts a significant impact on stabilizing mitochondrial electron transport and reducing ROS generation under salt stress (Zsigmond et al. 2008, 2012).

Interestingly, the absence of PPR40 protein in the *ppr40-1* mutant resulted in compromised mitochondrial electron transport through Complex III, leading to heightened ROS production, increased H₂O₂ content, and hypersensitivity to ABA (Zsigmond et al. 2008). The role of hydrogen peroxide as a mediator of ABA signals in guard cells, together with cytosolic Ca²⁺, acting as a second messenger to coordinate ion transport and facilitate stomatal closure under drought stress, further emphasizes the importance of PPR40 in drought response (Zhang et al. 2001; Kwak 2003; Postiglione and Muday 2020). Additionally, the activation of NADPH-oxidases (Respiratory Burst Oxidase Homologs, RBOH) by SnRK2-mediated phosphorylation was shown to control ROS accumulation in response to ABA (Kwak 2003; Sirichandra et al. 2009). A recent discovery suggesting that mitochondria and chloroplasts serve as significant sources of ABA-generated H₂O₂ in guard cells, and that mitochondria-derived H₂O₂ is responsible for enhancing ABA sensitivity and promoting ABA-triggered stomatal closure (Postiglione and Muday 2023). These data are in line with our results obtained with the *ppr40* mutants and confirm the relevance of PPR40-modulated mitochondrial functions in ABA signaling. Hence, the enhanced ABA sensitivity observed in the *ppr40-1* mutant may be attributed to the increased H₂O₂ production resulting from the damaged mitochondrial electron transport, ultimately promoting stomatal closure (Figure 24) (Zsigmond et al. 2008). Also, stress priming or pre-exposure to mild stress, can enhance a plant's adaptation to future events and the development of stress memory. Due the production of H₂O₂ in *ppr40* mutants, plants might have developed adaptive mechanisms to cope with drought stress more efficiently (Lagiotis et al 2023)

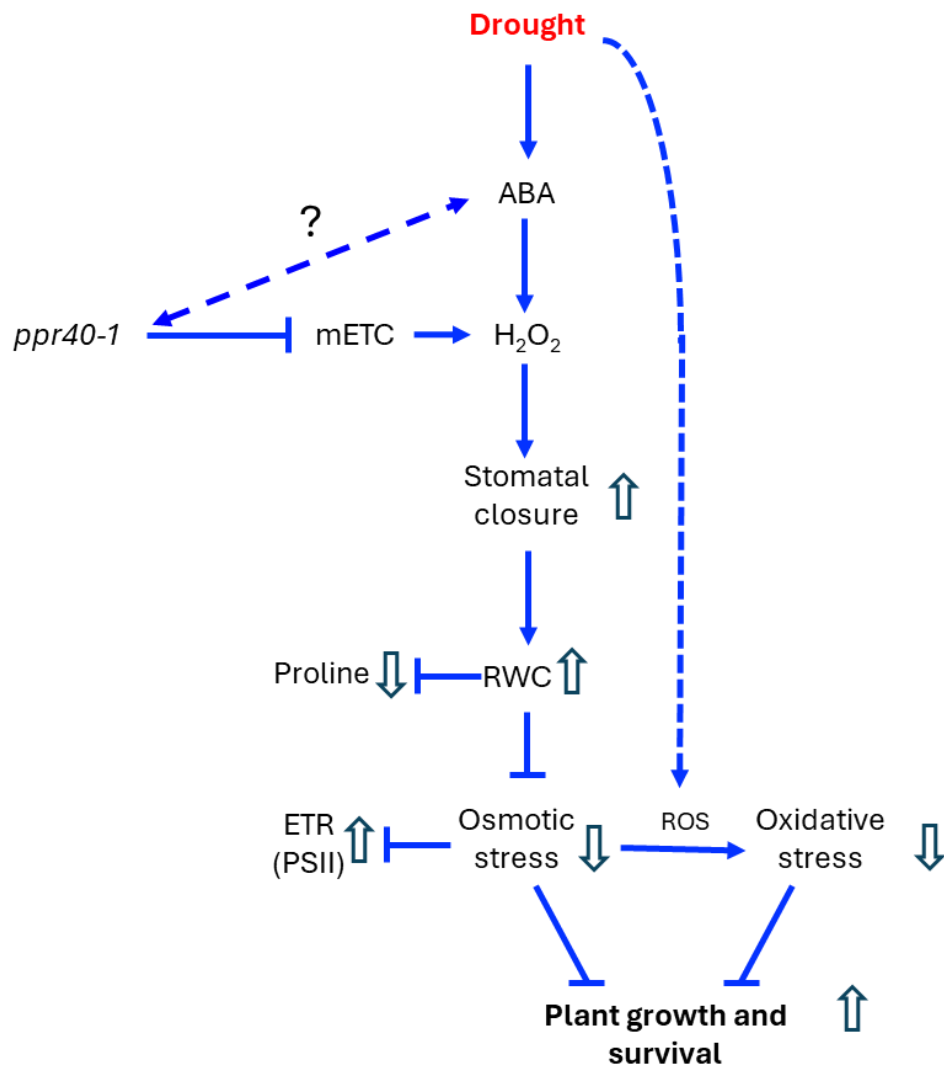


Figure 24. Model of PPR40 action in drought responses of Arabidopsis plants. PPR40 is associated with Complex III in mETC and can downregulate ABA signaling in dehydrating plants as it stabilizes electron transport and suppresses ROS generation. ABA-induced stomata closure is faster in the *ppr40-1* mutant reducing water loss during drought and leading to higher RWC that diminishes osmotic pressure. Reduced proline accumulation in *ppr40-1* can be the consequence of higher RWC and lower osmotic pressure. Lower osmotic and oxidative stress in drought-stressed *ppr40-1* can alleviate inhibition of photosynthetic ETR and contribute to enhanced viability and growth of drought-stressed *ppr40-1* plants. Small arrows indicate enhanced or diminished features in water-stressed *ppr40-1* mutant.

Mitochondria play a pivotal role in influencing various metabolic and hormonal signaling pathways, thus modulating physiological processes, ROS homeostasis, and gene expression patterns (Rhoads and Subbaiah 2007; Møller et al. 2021b). Studies on mutants with mitochondrial defects have revealed altered ABA sensitivity, particularly during germination, which is an energy-demanding process (Wang et al. 2014; Huang et al. 2016). Furthermore,

mitochondrial ROS has been shown to impact plant hormone signaling, especially abscisic acid and auxin. For instance, the hot ABA-deficiency suppressor 2 (HAS2) encodes a PPR protein responsible for editing a cytochrome c-heme lyase subunit coding RNA. The *has2* mutation has increased respiration and H₂O₂ production, leading to enhanced ABA sensitivity of stomatal closure and increased drought tolerance (Sechet et al. 2015). Similarly, SLG1, another PPR protein involved in RNA editing of *nad3*, a key component of Complex I in the mitochondrial electron transport chain, displays impaired electron transport and excessive H₂O₂ production, resulting in ABA hypersensitivity, faster stomatal closure, and improved drought tolerance (Yuan and Liu 2012). The parallel phenotypic characteristics observed in both *slg1* and *ppr40-1* mutants, along with their enhancement of ABA responses, support the idea that mutations affecting Complex I or Complex III in the mitochondrial electron transport chain led to similar phenotypes, ultimately promoting enhanced drought tolerance.

The two insertion mutants *ppr40-1* and *ppr40-2* were previously identified as representing null and leaky mutations, respectively. Their differential ABA hypersensitivity observed in germination assays suggests that the two alleles may exert varying degrees of influence on ABA signaling (Zsigmond et al. 2008). The faster stomatal closure observed in these mutants enables them to retain higher leaf water content during drought conditions, thus reducing osmotic and oxidative stress (Bharath et al. 2021). Consequently, the improved drought tolerance in the *ppr40-1* and *ppr40-2* mutants correlates with earlier observations and confirms *ppr40-1* as a strong, while *ppr40-2* is a weak mutant allele.

Moreover, the higher water content in drought conditions influences various physiological and molecular parameters, ultimately impacting the stress tolerance of plants. Proline accumulation, a characteristic metabolic response to high osmotic conditions with protective effects against drought stress, was found to be lower in the *ppr40-1* mutant compared to *ppr40-2* and wild type plants. This difference could be attributed to the higher relative water content of *ppr40-1* and *ppr40-2* mutants under water-deprivation conditions. The negative correlation between leaf water content and proline accumulation aligns with previous studies and supports our findings (Sperdouli and Moustakas 2012). Moreover, transcript levels of the ABA-induced *P5CS1* gene were lower in the *ppr40* mutants compared to Col-0 plants under water deprivation, which correlated with the inferior proline accumulation observed. Interestingly, higher proline content was detected in *ppr40* mutants under well-watered conditions, possibly due to their ABA hypersensitivity.

Photosynthesis is one of the most sensitive metabolic processes to water deprivation, significantly affected in our water-stressed plants. However, time-course analysis of

chlorophyll fluorescence indicated that the decline in PSII quantum yield (Fv/Fm) was slower in *ppr40-1* and *ppr40-2* mutants compared to Col-0 wild-type plants, indicating a more stable photosynthetic process in the mutants (Figure 18). Furthermore, the electron transport rate of PSII, measured at different light intensities in water-limited conditions, was significantly higher in *ppr40-1* and to a lesser extent in *ppr40-2* than in wild type plants (Figure 19). These observations suggest that drought-induced photo-damage of PSII was alleviated in *ppr40* mutants, which is consistent with their reduced oxidative damage and moderate inhibition of photosynthetic processes.

Mitochondria and chloroplasts have a close interaction in various metabolic and signaling pathways, which adds complexity to drought tolerance mechanisms (Blanco et al. 2014; Van Aken 2021). *Alternative oxidases (AOX)* play a vital role in non-energy conserving electron transport pathways that help stabilize energy balance during stress, such as drought (Vanlerberghe et al. 2016). Our data revealed significantly higher *AOX1a* and *AOX1d* transcript levels in drought-treated *ppr40* mutants compared to wild type plants, suggesting that these mutants experienced limited stress and had less activated non-phosphorylating respiratory pathways (Figure 22c).

In conclusion, our study has provided valuable insights into the multifaceted role of the mitochondrial PPR40 protein in modulation of drought tolerance in Arabidopsis plants. *PPR40's* influence on various physiological and molecular processes, including ABA sensitivity, proline accumulation, photosynthetic stability, ROS generation, and gene expression patterns, contributes to responses to water deprivation, as observed in the *ppr40* mutants. These findings advance our understanding of the intricate mechanisms underlying plant stress regulation and emphasize the potential of PPR40 as a promising target for engineering to improve drought tolerance in crops, addressing the challenges of water scarcity. However, it is important to acknowledge that some aspects remain to be fully explored. For instance, a more comprehensive understanding of the specific downstream targets and signaling pathways regulated by PPR40, as well as its potential interaction with other proteins, would provide valuable insights into the underlying molecular mechanisms. Additionally, investigating the interplay between PPR40 and other stress-responsive pathways, such as the role of ABA and ROS signaling in drought responses, could reveal intricate crosstalk and synergistic effects. Moreover, expanding the analysis to other plant species and agricultural crops would be instrumental in assessing the broader applicability of PPR40-based strategies for enhancing drought tolerance.

The findings presented in this thesis contribute significantly to our knowledge of the molecular and physiological mechanisms governing drought tolerance in plants. The identification of *PPR40* as a possible key player in these processes opens new avenues for targeted genetic engineering and breeding approaches aimed at developing drought-tolerant crops, which are crucial for ensuring food security and sustainable agriculture in the face of global climate change. By unraveling the complex interplay of mitochondrial function, ABA signaling, and stress responses, this research paves the way for future investigations and applications in crop improvement and environmental sustainability.

6. Summary

Climate change poses adverse effects on plants, particularly crucial agricultural crops. One of the most pressing concerns is drought which can cause severe food scarcity in the world; therefore, it is necessary to understand the intricate plant mechanisms to develop resilient crop varieties. The findings presented in this thesis provide significant insights into the role of PPR40 in enhancing drought tolerance in Arabidopsis plants. Through a comprehensive analysis of various physiological, biochemical, and molecular parameters, we have demonstrated the role of PPR40 in conferring resilience to water stress.

The Arabidopsis thaliana *ppr40-1* mutant showed hypersensitivity to ABA, salt and sugar in germination assays, was identified in a T-DNA insertion mutagenesis program. The knock-out mutant plants exhibit a semi-dwarf growth phenotype. In addition, another allele was identified, *ppr40-2*, whose mutation did not completely abolish the *PPR40* gene function but resulted in a phenotype intermediate between *ppr40-1* and the wild type. These mutations in the *PPR40* gene affect mitochondrial electron transport chain reducing electron transport rates. Our investigation began by characterizing the *ppr40* mutant's response to drought conditions. The ABA hypersensitivity is correlated with improved survival rates in water-limited conditions, as the *ppr40-1* mutant showed significantly higher survival rates compared to Col-0 wild-type plants, while the *ppr40-2* mutant exhibited intermediate survival rates.

Complex phenotyping of the *ppr40* mutants in an automatic plant phenotyping platform provided valuable information on their growth and morphology in well-watered and water-limited conditions. Under standard growth conditions, the *ppr40-1* mutant showed semi-dwarf phenotype and reduced growth rates when compared to Col-0 (wild type) and *ppr40-2* mutant. However, under water stress, the *ppr40* mutants exhibited delayed declines in rosette size and sustained their viability for longer periods compared to wild-type plants. The analysis of hue ratios and slenderness of leaves further supported the superior tolerance of the *ppr40* mutants to water deprivation, as their rosette morphology was better preserved during water stress.

We further investigated the stability of photosynthesis in the *ppr40* mutants under drought conditions. Chlorophyll fluorescence analysis indicated that photosynthetic electron transport remained functional for more extended periods in the drought-stressed *ppr40* mutants compared to wild-type plants. The maximum quantum yield analyzed under automatic phenotypic system, dropped faster in Col-0 when compared to *ppr-40* mutants under water deficit conditions, again supporting our results.

The higher water content during drought conditions affects a range of physiological parameters, eventually influencing the stress tolerance of plants. Physiological parameters, such as Relative water content, proline accumulation, and MDA revealed important insights into the drought tolerance mechanisms of the *ppr40* mutants. *ppr40* mutants showed better water retention capabilities, with significantly reduced RWC reductions under water stress compared to wild-type plants, due to faster stomata closure in *ppr40* mutants. Proline accumulation, a well-known response to water deprivation in plants, was also higher in the Col-0 when compared to *ppr40* mutants, suggesting that these mutants experience less stress. The lower level of *P5CS1* gene expression in *ppr40* mutants correlates well with compromised proline accumulation. Additionally, we observed reduced oxidative damage in the *ppr40* mutants, as evidenced by lower lipid peroxidation rates (MDA levels) and attenuated ROS-induced gene activation.

The modulation of drought-induced gene expression, ABA-responsive genes, and stress-responsive Alternative Oxidases (AOX) further highlights the role of *PPR40* in regulating plant responses to water stress. The *ppr40-1* mutant displayed significantly reduced transcript levels of the ABA-induced dehydrin gene *RAB18* under drought stress, with *ppr40-2* exhibiting intermediate expression compared to wild-type plants. Transcript levels of the ROS-induced gene regulator *ZAT12* were also significantly lower in *ppr40-1*, indicating attenuated activation of ROS-dependent gene expression under drought treatment. Expression analysis revealed lower *AOX1a* and *AOX1d* transcript levels in drought-induced *ppr40* mutants compared to wild type plants, suggesting that these mutants experienced limited stress and their non-phosphorylating respiratory pathways were less active. The expression levels of bZIP-type *ABF* transcription factors, which are key regulators of ABA-induced transcription and showed similar patterns to *AOX* genes. These lower levels in *ppr40* mutants were basically because the decreased water reduction prevented dehydration hence there was lower accumulation of reactive oxygen species and lower oxidative stress. We examined the transcript levels of specific genes involved in auxin, salicylic acid (SA), and other hormone-related genes, but this effect was less pronounced or absent in the *ppr40* mutants.

Overall, the comprehensive analysis of the *ppr40* mutants revealed that *PPR40* can play a critical role in modulating drought tolerance through multiple interconnected mechanisms. The mutants exhibited improved water retention, reduced oxidative damage, and stabilized photosynthetic electron transport, resulting in better survival rates under water stress. These findings shed light on the complex interplay between ABA signaling, photosynthesis, ROS homeostasis, and stress-responsive gene regulation, all of which can be influenced by the absence of *PPR40* protein.

A deeper understanding of the function of PPR40 and related proteins in enhancing drought tolerance could have an impact on crop improvement. Such an understanding holds great promise for addressing escalating water scarcity and mitigating the adverse effects of climate change. Harnessing the potential of the PPR40 protein in ongoing plant breeding initiatives offers the opportunity to develop more resilient and productive crop varieties. Such efforts are key to strengthening future food security and promoting sustainable agricultural practices.

7. Összefoglaló

Az éghajlatváltozás következtében megjelenő káros környezeti változások számtalan negatív következménnyel járnak a növényekre, különösen a kulcsfontosságú mezőgazdasági növényekre. Az egyik legégetőbb probléma az aszály, amely súlyos élelmiszerhiányt okozhat a világon, ezért szükséges lehet megérteni a növények összetett védekezési mechanizmusait, hogy a későbbiekben ellenálló növényfajtákat fejleszthessünk ki. A jelen disszertációmban bemutatott eredmények betekintést nyújtanak az *Arabidopsis PPR40* fehérje szerepére a szárazságtűrés szabályozásában. A különböző fiziológiai, biokémiai és molekuláris biológiai paraméterek átfogó elemzésével bemutatjuk a *PPR40* fontos szerepét a vízhiánnyal szembeni ellenálló képesség elősegítésében.

Az *Arabidopsis thaliana ppr40-1* mutáns vonalat egy T-DNS inszerciós mutagenézis programban azonosították. A mutáns csíráztási tesztekben túlérzékenységet mutatott abszizin savval (ABS), sóval és cukorral szemben. A funkcióvesztéses *ppr40-1* mutáns növények „félíg törpe” növekedési fenotípussal rendelkeznek. Ezen kívül egy másik allélt is sikerült azonosítani: a *ppr40-2*-t, amely esetében mutáció nem szüntette meg teljesen a *PPR40* gén funkcióját, ami a *ppr40-1* és a vad típus közti fenotípust eredményezett. A *PPR40* gén ezen mutációi képesek befolyásolni a mitokondriális elektrontranszportot, csökkentve annak hatékonyságát.

A kutatásaink során a *ppr40* mutánsok szárazságra adott válaszainak vizsgálatára fókuszáltunk. A *ppr40-1* mutáns fokozott ABS érzékenységet, míg a *ppr40-2* egy átmeneti fenotípust mutatott a vad típushoz képest, ami gyorsabban sztómazáródáshoz és csökkent vízvesztéshez vezetett. Az ABS érzékenység kapcsolatban állt a szárazság tűrő képesség javulásával, mivel a *ppr40-1* mutánsban a túlélési arány jelentősen magasabb volt a vad típusú növényekhez képest. A *ppr40-2* mutáns esetében egy átmeneti, kevésbé kiugró különbséget figyeltünk meg a túlélési arányban, ami megerősítette az ABS érzékenység és szárazságtűrés közötti kapcsolatot.

Automatizált növény fenotipizáló rendszer segítségével végzett kísérletek segítségével a *ppr40* mutánsok növekedéséről, morfológiai és fonoszintézis változásairól szereztünk értékes információkat locsolt illetve vízhiányos körülmények között. Jó öntözési feltételek mellett a *ppr40-1* mutáns a korábról ismert kis növekedésű fenotípust mutatta kisebb rozetta mérettel, míg a *ppr40-2* egy a vad típusú növényekhez hasonló növekedést mutatott. Vízmegvonás következtében a *ppr40* mutánsok rozetta mérete lassabban csökkent, és életképességüket is hosszabb idejig képesek voltak fenntartani a vad típusú növényekhez viszonyítva. A színtónus arányok és a levél karcsúság változásának adatai szintén megerősítették a *ppr40* mutánsok

szárazság tűréssel összefüggő jobb eredményeit, mivel rozetta morfológiájuk jobban megőrződött vízhiányos körülmények között. A fotoszintézis stabilitását is vizsgáltuk *ppr40* mutánsoknál a komplex fenotipizáló rendszer segítségével vízmegvonásos után. A klorofill fluoreszcencia elemzése azt mutatta, hogy a fotoszintetikus elektrontranszport hosszabb ideig maradt aktív a *ppr40* mutánsoknál a vad típusú növényekhez képest, és a maximális kvantumhozam is lassabban csökkent a mutánsokban a vad típushoz képest. Ezek az eredmények alátámasztják a *ppr40* mutánsok szárazsággal szembeni megnövekedett toleranciáját.

A szárazság idején tapasztalható magasabb víztartalom számos élettani paraméterre hatással van, és befolyásolhatja a növények stressztűrő képességét. Az olyan fiziológiai paraméterek, mint például a relatív víztartalom (RWC), a prolin felhalmozódása és a lipidek oxidációs állapota fontos betekintést engedtek a *ppr40* mutánsok szárazságtűrési mechanizmusába. A *ppr40* mutánsok jobb vízmegtartó képességgel rendelkeznek: vízmegvonás esetén a vad típusú növényekhez képest szignifikánsan nagyobb RWC értékeket mutattak, ami a gyorsabb sztómazáródására vezethető vissza. A prolin felhalmozódás jellemző a vízhiányos növényekben. A vízmegvonásnak kitett növények prolin tartalma alacsonyabb volt a *ppr40* mutánsokban mint a vad típusú növényekben, ami jelzi, hogy a mutánsokra kevésbé hatott a vízmegvonás miatt kialakult ozmotikus stressz. A *P5CS1* gén expressziójának alacsonyabb szintje a *ppr40* mutánsokban összefügg a megváltozott prolin felhalmozódással. Emellett csökkent oxidatív károsodást figyeltünk meg *ppr40* mutánsokban, amit az alacsonyabb lipidek oxidációs szintje (MDA-szint) és a kisebb ROS-indukált génkifejeződés bizonyított.

A *ppr40-1* mutánsban jelentősen alacsonyabb volt az ABS által indukált *RAB18* dehidrin gén kifejeződése vízhiány során, míg a *ppr40-2* esetében ez a különbség kisebb volt. Hasonló mintázatot mutatott az oxidatív stresszválaszt szabályozó *ZAT12* expressziója, amely szignifikánsan alacsonyabb volt a *ppr40-1* mutánsban a vad típushoz képest. A mitokondriumban lokalizált alternatív oxidázokat kódoló *AOX1a* és *AOX1d* gének expressziója szintén alacsonyabb volt a *ppr40* mutánsokban a vad típusú növényekhez képest, utalva a nem foszforiláló légzési útvonaluk csökkent aktivitására. Az ABS-indukált transzkripciót szabályozó bZIP típusú *ABF* transzkripciós faktorok (*ABF2* és *ABF3*) expressziós szintjei hasonló mintázatot mutattak az *AOX* génekhez. A *ppr40* mutánsokban ezek az alacsonyabb expressziós szintek azért alakulhattak ki, mert a csökkent vízvesztés megakadályozta a kiszáradást, így alacsonyabb volt a reaktív oxigénfajták felhalmozódása és az oxidatív stressz. Megvizsgáltuk különböző növényi hormonokhoz kapcsolt jelátviteli utakban részt vevő gének kifejeződését is, melyek esetében alacsonyabb indukciót tapasztaltunk mutánsokban a vad

típushoz képest. Ezek az eredmények arra utalnak, hogy a PPR40 közvetve befolyásolhatja az etilénnel, jázmonáttal, brassinoszteroidokkal és citokininnel kapcsolatos útvonalakat is.

Összességében a *ppr40* mutánsok részletes elemzése kimutatta, hogy a PPR40 fontos szerepet játszhat az szárazság tűrés szabályozásában. A mutánsok jobb vízmegtartással rendelkeztek, csökkentett oxidatív károsodást és stabiliabb a fotoszintetikus elektrontranszportot mutattak, ami jobb túlélési arányt eredményezett. Ezek az eredmények rávilágítanak az ABS-jelátvitel, a fotoszintézis, a ROS-homeosztázis és a stressz által befolyásolt génszabályozás közötti összetett kölcsönhatásra, amelyenekre hatással lehet a PPR40 hiánya.

A PPR40 és a hozzá hasonló funkcióval rendelkező fehérjék szerepének jobb megértése hozzájárulhat a szárazságtűrés javítását célzó új biotechnológiai stratégiák kidolgozását. Az általunk vizsgált PPR40 fehérjében rejlő lehetőségek kiaknázása a növénynevelési programokban lehetőséget teremthet rugalmasabb és produktívabb fajták kifejlesztésében, segítve a jövőbeni élelmezésbiztonságot és a fenntartható mezőgazdaságot.

8. Acknowledgment

First and foremost, I would like to express my deepest gratitude to my exceptional supervisor, Dr. **Laura Zsigmond**. Her unswerving support, guidance, and profound knowledge have shaped the trajectory of my doctoral research. Her dedication to mentoring and genuine passion for academic exploration have inspired me to strive for excellence.

I am indebted to my esteemed head of the laboratory, Dr. **László Szabados**, for his contributions to my research journey. His insightful feedback, encouragement, and commitment to fostering a stimulating research environment have played a pivotal role in my growth as a researcher.

A special mention goes to Dr. **Gábor Rigó**, whose guidance and support have been truly invaluable. His patience, competence, and willingness to share his knowledge have consistently pushed me beyond my limits and helped me overcome research challenges.

To my fellow lab members, **Annamária Király, Dániel Benyó, Atina Martics, Sahilu Ahmad Rabilu, Melvin Prasad, Balla Mariann, and Ildikó Valkai**. I extend my sincere thanks for their intellectual discussions and mutual support. The shared experiences and diverse perspectives within our lab have enriched my research experience immeasurably.

Gellért Czékus, words cannot adequately express my gratitude for your enduring belief in me, countless sacrifices, and constant support. Your love, understanding, and encouragement have been my anchor, and I am truly blessed to have you by my side.

I would like to express my heartfelt gratitude to my dear friend, **Poonam Nebhnani**. Her support, encouragement, and the cherished moments we shared during this journey have provided inspiration during challenging times. I would also like to acknowledge the friendship and support of **Dér László, Neha Sahu, Gaurav Sharma, Bayan, Abhishek, and Anish**. Your presence, conversations, and shared experiences have brought immense joy and camaraderie into my life.

Furthermore, I would like to thank **HUN-REN Biological Research Centre Szeged** and the **University of Szeged** for providing me with the necessary resources and facilities to conduct my research. I am also grateful to **NKFIH K128728, FK128920, K143620, GINOP-2.3.3-15-2016-00023** for their financial support throughout my doctoral studies.

Finally, I extend my deepest appreciation to my parents and family members for their unconditional love and credence in my abilities. Your constant encouragement and sacrifices have been the driving force behind my accomplishments.

To each person mentioned above, and to those whose names may have unintentionally been omitted, please accept my heartfelt gratitude for your contributions, support, and belief in my abilities. This dissertation would not have been possible without your invaluable assistance and encouragement.

Thank you all from the bottom of my heart.

9. References

- Ábrahám E, Hourton-Cabassa C, Erdei L, Szabados L (2010) Methods for Determination of Proline in Plants. pp 317–331
- Ahluwalia O, Singh PC, Bhatia R (2021a) A review on drought stress in plants: Implications, mitigation and the role of plant growth promoting rhizobacteria. *Resources, Environment and Sustainability* 5:100032. <https://doi.org/10.1016/j.resenv.2021.100032>
- Ahluwalia O, Singh PC, Bhatia R (2021b) A review on drought stress in plants: Implications, mitigation and the role of plant growth promoting rhizobacteria. *Resources, Environment and Sustainability* 5:100032. <https://doi.org/10.1016/j.resenv.2021.100032>
- Alseekh S, Aharoni A, Brotman Y, et al (2021) Mass spectrometry-based metabolomics: a guide for annotation, quantification and best reporting practices. *Nat Methods* 18:747–756
- Alvarez ME, Saviouré A, Szabados L (2022) Proline metabolism as regulatory hub. *Trends Plant Sci* 27:39–55. <https://doi.org/10.1016/j.tplants.2021.07.009>
- An Y, McDowell JM, Huang S, et al (1996) Strong, constitutive expression of the *Arabidopsis* *ACT2/ACT8* actin subclass in vegetative tissues. *The Plant Journal* 10:107–121. <https://doi.org/10.1046/j.1365-313X.1996.10010107.x>
- Andrási N, Rigó G, Zsigmond L, et al (2019) The mitogen-activated protein kinase 4-phosphorylated heat shock factor A4A regulates responses to combined salt and heat stresses. *J Exp Bot* 70:4903–4918
- Awlia M, Nigro A, Fajkus J, et al (2016) High-Throughput Non-destructive Phenotyping of Traits that Contribute to Salinity Tolerance in *Arabidopsis thaliana*. *Front Plant Sci* 7:. <https://doi.org/10.3389/fpls.2016.01414>
- Ayaydin F, Bíró J, Domoki M, et al (2015) *Arabidopsis* NAP-related proteins (NRPs) are soluble nuclear proteins immobilized by heat. *Acta Physiol Plant* 37:3. <https://doi.org/10.1007/s11738-014-1753-z>
- Baker NR (2008) Chlorophyll Fluorescence: A Probe of Photosynthesis In Vivo. *Annu Rev Plant Biol* 59:89–113. <https://doi.org/10.1146/annurev.arplant.59.032607.092759>
- Barrs HD, Weatherley PE (1962) A Re-Examination of the Relative Turgidity Technique for Estimating Water Deficits in Leaves. *Aust J Biol Sci* 15:413. <https://doi.org/10.1071/BI9620413>
- Besseau S, Li J, Palva ET (2012) WRKY54 and WRKY70 co-operate as negative regulators of leaf senescence in *Arabidopsis thaliana*. *J Exp Bot* 63:2667–2679. <https://doi.org/10.1093/jxb/err450>
- Bharath P, Gahir S, Raghavendra AS (2021) Abscisic Acid-Induced Stomatal Closure: An Important Component of Plant Defense Against Abiotic and Biotic Stress. *Front Plant Sci* 12:. <https://doi.org/10.3389/fpls.2021.615114>
- Blanco NE, Guinea-Díaz M, Whelan J, Strand Å (2014) Interaction between plastid and mitochondrial retrograde signalling pathways during changes to plastid redox status. *Philosophical Transactions of the Royal Society B: Biological Sciences* 369:20130231

- Braun H-P (2020) The Oxidative Phosphorylation system of the mitochondria in plants. *Mitochondrion* 53:66–75. <https://doi.org/10.1016/j.mito.2020.04.007>
- Bryant C, Fuenzalida TI, Brothers N, et al (2021) Shifting access to pools of shoot water sustains gas exchange and increases stem hydraulic safety during seasonal atmospheric drought. *Plant Cell Environ* 44:2898–2911. <https://doi.org/10.1111/pce.14080>
- Chen J, Nolan T, Ye H, et al (2017) Arabidopsis WRKY46, WRKY54 and WRKY70 Transcription Factors Are Involved in Brassinosteroid-Regulated Plant Growth and Drought Response. *Plant Cell tpc.00364.2017-tpc.00364.2017*. <https://doi.org/10.1105/tpc.17.00364>
- Chen J, Zhang J, Kong M, et al (2021a) More stories to tell: NONEXPRESSOR OF PATHOGENESIS-RELATED GENES1, a salicylic acid receptor. *Plant Cell Environ* 44:1716–1727
- Chen X, Ding Y, Yang Y, et al (2021b) Protein kinases in plant responses to drought, salt, and cold stress. *J Integr Plant Biol* 63:53–78. <https://doi.org/10.1111/jipb.13061>
- Cheng S, Gutmann B, Zhong X, et al (2016) Redefining the structural motifs that determine RNA binding and RNA editing by pentatricopeptide repeat proteins in land plants. *The Plant Journal* 85:532–547
- Cheol Park H, Cha J-Y, Yun D-J (2013) Roles of YUCCAs in auxin biosynthesis and drought stress responses in plants. *Plant Signal Behav* 8:e24495–e24495. <https://doi.org/10.4161/psb.24495>
- Choudhury FK, Rivero RM, Blumwald E, Mittler R (2017) Reactive oxygen species, abiotic stress and stress combination. *The Plant Journal* 90:856–867. <https://doi.org/10.1111/tpj.13299>
- Clifton R, Millar AH, Whelan J (2006a) Alternative oxidases in Arabidopsis: a comparative analysis of differential expression in the gene family provides new insights into function of non-phosphorylating bypasses. *Biochimica et Biophysica Acta (BBA)-Bioenergetics* 1757:730–741
- Clifton R, Millar AH, Whelan J (2006b) Alternative oxidases in Arabidopsis: A comparative analysis of differential expression in the gene family provides new insights into function of non-phosphorylating bypasses. *Biochimica et Biophysica Acta (BBA) - Bioenergetics* 1757:730–741. <https://doi.org/10.1016/j.bbabi.2006.03.009>
- Coego A, Brizuela E, Castillejo P, et al (2014) TRANSPLANTA Consortium The TRANSPLANTA collection of Arabidopsis lines: A resource for functional analysis of transcription factors based on their conditional overexpression. *Plant J* 77:944–953
- Considine MJ, Foyer CH (2014) Redox Regulation of Plant Development. *Antioxid Redox Signal* 21:1305–1326. <https://doi.org/10.1089/ars.2013.5665>
- Daszkowska-Golec A, Szarejko I (2013) Open or Close the Gate – Stomata Action Under the Control of Phytohormones in Drought Stress Conditions. *Front Plant Sci* 4:. <https://doi.org/10.3389/fpls.2013.00138>
- Davletova S, Schlauch K, Coutu J, Mittler R (2005) The Zinc-Finger Protein Zat12 Plays a Central Role in Reactive Oxygen and Abiotic Stress Signaling in Arabidopsis . *Plant Physiol* 139:847–856. <https://doi.org/10.1104/pp.105.068254>
- Demidchik V (2015) Mechanisms of oxidative stress in plants: From classical chemistry to cell biology. *Environ Exp Bot* 109:212–228. <https://doi.org/10.1016/j.envexpbot.2014.06.021>
- Ding Y-H, Liu N-Y, Tang Z-S, et al (2006) Arabidopsis GLUTAMINE-RICH PROTEIN23 Is Essential for Early Embryogenesis and Encodes a Novel Nuclear PPR Motif Protein That

- Interacts with RNA Polymerase II Subunit III. *Plant Cell* 18:815–830.
<https://doi.org/10.1105/tpc.105.039495>
- Duby G, Boutry M (2002) Mitochondrial protein import machinery and targeting information. *Plant Science* 162:477–490
- Dutilleul C, Garmier M, Noctor G, et al (2003) Leaf mitochondria modulate whole cell redox homeostasis, set antioxidant capacity, and determine stress resistance through altered signaling and diurnal regulation. *Plant Cell* 15:1212–1226
- Faragó D, Zsigmond L, Benyó D, et al (2022) Small paraquat resistance proteins modulate paraquat and ABA responses and confer drought tolerance to overexpressing Arabidopsis plants. *Plant Cell Environ* 45:1985–2003. <https://doi.org/10.1111/pce.14338>
- Farooq M, Basra SMA, Wahid A, et al (2009) Improving the Drought Tolerance in Rice (*Oryza sativa* L.) by Exogenous Application of Salicylic Acid. *J Agron Crop Sci* 195:237–246.
<https://doi.org/10.1111/j.1439-037X.2009.00365.x>
- Finkelstein R (2013a) Abscisic Acid Synthesis and Response. *Arabidopsis Book* 11:e0166.
<https://doi.org/10.1199/tab.0166>
- Finkelstein R (2013b) Abscisic acid synthesis and response. *The Arabidopsis book/American society of plant biologists* 11:
- Fortunato S, Lasorella C, Tadini L, et al (2022) GUN1 involvement in the redox changes occurring during biogenic retrograde signaling. *Plant Science* 320:111265
- Gaion LA, Carvalho RF (2021) Stomatal response to drought is modulated by gibberellin in tomato. *Acta Physiol Plant* 43:129
- Gray MW, Burger G, Lang BF (1999) Mitochondrial evolution. *Science* (1979) 283:1476–1481
- Hammani K, Gobert A, Hleibieh K, et al (2011) An *Arabidopsis* Dual-Localized Pentatricopeptide Repeat Protein Interacts with Nuclear Proteins Involved in Gene Expression Regulation. *Plant Cell* 23:730–740. <https://doi.org/10.1105/tpc.110.081638>
- Hashimoto M, Endo T, Peltier G, et al (2003) A nucleus-encoded factor, CRR2, is essential for the expression of chloroplast *ndhB* in *Arabidopsis*. *The Plant Journal* 36:541–549.
<https://doi.org/10.1046/j.1365-313X.2003.01900.x>
- Hayes ML, Santibanez PI (2020) A plant pentatricopeptide repeat protein with a DYW-deaminase domain is sufficient for catalyzing C-to-U RNA editing in vitro. *Journal of Biological Chemistry* 295:3497–3505. <https://doi.org/10.1074/jbc.RA119.011790>
- He P, Shan L, Sheen J (2007) Elicitation and suppression of microbe-associated molecular pattern-triggered immunity in plant-microbe interactions. *Cell Microbiol* 9:1385–1396.
<https://doi.org/10.1111/j.1462-5822.2007.00944.x>
- He X, Estes L, Konar M, et al (2019) Integrated approaches to understanding and reducing drought impact on food security across scales. *Curr Opin Environ Sustain* 40:43–54
- Heath RL, Packer L (1968) Photoperoxidation in isolated chloroplasts. *Arch Biochem Biophys* 125:189–198. [https://doi.org/10.1016/0003-9861\(68\)90654-1](https://doi.org/10.1016/0003-9861(68)90654-1)
- Hou Q, Ufer G, Bartels D (2016) Lipid signalling in plant responses to abiotic stress. *Plant Cell Environ* 39:1029–1048. <https://doi.org/10.1111/pce.12666>

- Huang H, Ullah F, Zhou D-X, et al (2019) Mechanisms of ROS regulation of plant development and stress responses. *Front Plant Sci* 10:800
- Huang S, Van Aken O, Schwarzländer M, et al (2016) The Roles of Mitochondrial Reactive Oxygen Species in Cellular Signaling and Stress Response in Plants. *Plant Physiol* 171:1551–1559. <https://doi.org/10.1104/pp.16.00166>
- Ichinose M, Tasaki E, Sugita C, Sugita M (2012) A PPR-DYW protein is required for splicing of a group II intron of *cox1* pre-mRNA in *Physcomitrella patens*. *The Plant Journal* 70:271–278. <https://doi.org/10.1111/j.1365-313X.2011.04869.x>
- Jiang J, Ma S, Ye N, et al (2017) WRKY transcription factors in plant responses to stresses. *J Integr Plant Biol* 59:86–101
- Jiang S-C, Mei C, Liang S, et al (2015) Crucial roles of the pentatricopeptide repeat protein SOAR1 in Arabidopsis response to drought, salt and cold stresses. *Plant Mol Biol* 88:369–385
- Jones A (2000) Does the plant mitochondrion integrate cellular stress and regulate programmed cell death? *Trends Plant Sci* 5:225–230
- Julkowska MM, Saade S, Agarwal G, et al (2019) MVApp—Multivariate Analysis Application for Streamlined Data Analysis and Curation. *Plant Physiol* 180:1261–1276. <https://doi.org/10.1104/pp.19.00235>
- Koncz C, Németh K, Rédei GP, Schell J (1992) T-DNA insertional mutagenesis in Arabidopsis. *Plant Mol Biol* 20:963–976
- Koussevitzky S, Nott A, Mockler TC, et al (2007) Signals from chloroplasts converge to regulate nuclear gene expression. *Science* 316:715–719
- Kuromori T, Seo M, Shinozaki K (2018) ABA Transport and Plant Water Stress Responses. *Trends Plant Sci* 23:513–522. <https://doi.org/10.1016/j.tplants.2018.04.001>
- Kwak JM (2003) NADPH oxidase AtrbohD and AtrbohF genes function in ROS-dependent ABA signaling in Arabidopsis. *EMBO J* 22:2623–2633. <https://doi.org/10.1093/emboj/cdg277>
- Lagiotis G, Madesis P, Stavridou E, (2023) Echoes of a Stressful Past: Abiotic Stress Memory in Crop Plants towards Enhanced Adaptation. *Agriculture* , 13, 2090. <https://doi.org/10.3390/agriculture13112090>
- Laluk K, AbuQamar S, Mengiste T (2011) The Arabidopsis Mitochondria-Localized Pentatricopeptide Repeat Protein PGN Functions in Defense against Necrotrophic Fungi and Abiotic Stress Tolerance . *Plant Physiol* 156:2053–2068. <https://doi.org/10.1104/pp.111.177501>
- Leaver CJ, Hack E, Forde BG (1983) [43] Protein synthesis by isolated plant mitochondria. In: *Methods in enzymology*. Elsevier, pp 476–484
- León J, Castillo MC, Coego A, et al (2014) Diverse functional interactions between nitric oxide and abscisic acid in plant development and responses to stress. *J Exp Bot* 65:907–921
- Li W, de Ollas C, Dodd IC (2018) Long-distance ABA transport can mediate distal tissue responses by affecting local ABA concentrations. *J Integr Plant Biol* 60:16–33. <https://doi.org/10.1111/jipb.12605>
- Lim C, Baek W, Jung J, et al (2015) Function of ABA in Stomatal Defense against Biotic and Drought Stresses. *Int J Mol Sci* 16:15251–15270. <https://doi.org/10.3390/ijms160715251>

- Liu L, Sonbol F-M, Huot B, et al (2016) Salicylic acid receptors activate jasmonic acid signalling through a non-canonical pathway to promote effector-triggered immunity. *Nat Commun* 7:13099. <https://doi.org/10.1038/ncomms13099>
- Liu S, Melonek J, Boykin LM, et al (2013) PPR-SMRs. *RNA Biol* 10:1501–1510. <https://doi.org/10.4161/rna.26172>
- Liu Y, He J, Chen Z, et al (2010) ABA overly-sensitive 5 (ABO5), encoding a pentatricopeptide repeat protein required for cis-splicing of mitochondrial nad2 intron 3, is involved in the abscisic acid response in Arabidopsis. *The Plant Journal* 63:749–765. <https://doi.org/10.1111/j.1365-313X.2010.04280.x>
- Livak KJ, Schmittgen TD (2001) Analysis of relative gene expression data using real-time quantitative PCR and the 2⁻ΔΔCT method. *methods* 25:402–408
- Logan DC (2006) The mitochondrial compartment. *J Exp Bot* 57:1225–1243
- Lu K, Li C, Guan J, et al (2022) The PPR-Domain Protein SOAR1 Regulates Salt Tolerance in Rice. *Rice* 15:62. <https://doi.org/10.1186/s12284-022-00608-x>
- Lurin C, Andreés C, Aubourg S, et al (2004a) Genome-Wide Analysis of Arabidopsis Pentatricopeptide Repeat Proteins Reveals Their Essential Role in Organelle Biogenesis[W]. *Plant Cell* 16:2089–2103. <https://doi.org/10.1105/tpc.104.022236>
- Lurin C, Andreés C, Aubourg S, et al (2004b) Genome-Wide Analysis of Arabidopsis Pentatricopeptide Repeat Proteins Reveals Their Essential Role in Organelle Biogenesis[W]. *Plant Cell* 16:2089–2103. <https://doi.org/10.1105/tpc.104.022236>
- Lv H-X, Huang C, Guo G-Q, Yang Z-N (2014) Roles of the nuclear-encoded chloroplast SMR domain-containing PPR protein SVR7 in photosynthesis and oxidative stress tolerance in Arabidopsis. *Journal of Plant Biology* 57:291–301. <https://doi.org/10.1007/s12374-014-0041-1>
- Macleán AE, Hayward JA, Huet D, et al (2022) The mystery of massive mitochondrial complexes: the apicomplexan respiratory chain. *Trends Parasitol* 38:1041–1052. <https://doi.org/10.1016/j.pt.2022.09.008>
- Makarevitch I, Waters AJ, West PT, et al (2015) Transposable Elements Contribute to Activation of Maize Genes in Response to Abiotic Stress. *PLoS Genet* 11:e1004915. <https://doi.org/10.1371/journal.pgen.1004915>
- Maurel C, Verdoucq L, Rodrigues O (2016) Aquaporins and plant transpiration. *Plant Cell Environ* 39:2580–2587. <https://doi.org/10.1111/pce.12814>
- Meinke DW, Cherry JM, Dean C, et al (1998) Arabidopsis thaliana: a model plant for genome analysis. *Science* (1979) 282:662–682
- Menezes-Silva PE, Sanglard LMVP, Ávila RT, et al (2017) Photosynthetic and metabolic acclimation to repeated drought events play key roles in drought tolerance in coffee. *J Exp Bot* 68:4309–4322. <https://doi.org/10.1093/jxb/erx211>
- Meyerowitz EM (1992) Introduction to the Arabidopsis genome. *Methods in Arabidopsis research* 100–118
- Millar AH, Whelan J, Soole KL, Day DA (2011a) Organization and Regulation of Mitochondrial Respiration in Plants. *Annu Rev Plant Biol* 62:79–104. <https://doi.org/10.1146/annurev-arplant-042110-103857>

- Millar AH, Whelan J, Soole KL, Day DA (2011b) Organization and Regulation of Mitochondrial Respiration in Plants. *Annu Rev Plant Biol* 62:79–104. <https://doi.org/10.1146/annurev-arplant-042110-103857>
- Mittler R, Blumwald E (2015) The Roles of ROS and ABA in Systemic Acquired Acclimation. *Plant Cell* 27:64–70. <https://doi.org/10.1105/tpc.114.133090>
- Møller IM, Jensen PE, Hansson A (2007) Oxidative Modifications to Cellular Components in Plants. *Annu Rev Plant Biol* 58:459–481. <https://doi.org/10.1146/annurev.arplant.58.032806.103946>
- Møller IM, Rasmusson AG, Van Aken O (2021a) Plant mitochondria—past, present and future. *The Plant Journal* 108:912–959
- Møller IM, Rasmusson AG, Van Aken O (2021b) Plant mitochondria – past, present and future. *The Plant Journal* 108:912–959. <https://doi.org/10.1111/tpj.15495>
- Mullineaux PM, Exposito-Rodriguez M, Laissue PP, Smirnov N (2018) ROS-dependent signalling pathways in plants and algae exposed to high light: Comparisons with other eukaryotes. *Free Radic Biol Med* 122:52–64. <https://doi.org/10.1016/j.freeradbiomed.2018.01.033>
- Munemasa S, Hauser F, Park J, et al (2015) Mechanisms of abscisic acid-mediated control of stomatal aperture. *Curr Opin Plant Biol* 28:154–162. <https://doi.org/10.1016/j.pbi.2015.10.010>
- Murayama M, Hayashi S, Nishimura N, et al (2012) Isolation of Arabidopsis ahg11, a weak ABA hypersensitive mutant defective in nad4 RNA editing. *J Exp Bot* 63:5301–5310. <https://doi.org/10.1093/jxb/ers188>
- Nakabayashi R, Saito K (2015) Integrated metabolomics for abiotic stress responses in plants. *Curr Opin Plant Biol* 24:10–16. <https://doi.org/10.1016/j.pbi.2015.01.003>
- Nakashima K, Yamaguchi-Shinozaki K, Shinozaki K (2014) The transcriptional regulatory network in the drought response and its crosstalk in abiotic stress responses including drought, cold, and heat. *Front Plant Sci* 5:. <https://doi.org/10.3389/fpls.2014.00170>
- Orimoloye IR, Belle JA, Orimoloye YM, et al (2022) Drought: A Common Environmental Disaster. *Atmosphere (Basel)* 13:111. <https://doi.org/10.3390/atmos13010111>
- Pandey S, Assmann SM (2004) The Arabidopsis Putative G Protein–Coupled Receptor GCR1 Interacts with the G Protein α Subunit GPA1 and Regulates Abscisic Acid Signaling. *Plant Cell* 16:1616–1632. <https://doi.org/10.1105/tpc.020321>
- Pavicic M, Mouhu K, Wang F, et al (2017) Genomic and phenomic screens for flower related RING type ubiquitin E3 ligases in Arabidopsis. *Front Plant Sci* 8:416
- Péret B, Swarup K, Ferguson A, et al (2012) AUX/LAX genes encode a family of auxin influx transporters that perform distinct functions during Arabidopsis development. *Plant Cell* 24:2874–2885
- Pérez-Salamó I, Papdi C, Rigó G, et al (2014) The Heat Shock Factor A4A Confers Salt Tolerance and Is Regulated by Oxidative Stress and the Mitogen-Activated Protein Kinases MPK3 and MPK6 . *Plant Physiol* 165:319–334. <https://doi.org/10.1104/pp.114.237891>
- Postiglione AE, Muday GK (2020) The Role of ROS Homeostasis in ABA-Induced Guard Cell Signaling. *Front Plant Sci* 11:. <https://doi.org/10.3389/fpls.2020.00968>
- Postiglione AE, Muday GK (2023) Abscisic acid increases hydrogen peroxide in mitochondria to facilitate stomatal closure. *Plant Physiol* 192:469–487. <https://doi.org/10.1093/plphys/kiac601>

- Prerostova S, Dobrev PI, Gaudinova A, et al (2018) Cytokinins: Their Impact on Molecular and Growth Responses to Drought Stress and Recovery in Arabidopsis. *Front Plant Sci* 9:. <https://doi.org/10.3389/fpls.2018.00655>
- Qiu T, Zhao X, Feng H, et al (2021) OsNBL3, a mitochondrion-localized pentatricopeptide repeat protein, is involved in splicing nad5 intron 4 and its disruption causes lesion mimic phenotype with enhanced resistance to biotic and abiotic stresses. *Plant Biotechnol J* 19:2277–2290
- Rhoads DM, Subbaiah CC (2007) Mitochondrial retrograde regulation in plants. *Mitochondrion* 7:177–194. <https://doi.org/10.1016/j.mito.2007.01.002>
- Rhoads DM, Umbach AL, Subbaiah CC, Siedow JN (2006) Mitochondrial reactive oxygen species. Contribution to oxidative stress and interorganellar signaling. *Plant Physiol* 141:357–366
- Riemann M, Dhakarey R, Hazman M, et al (2015) Exploring Jasmonates in the Hormonal Network of Drought and Salinity Responses. *Front Plant Sci* 6:. <https://doi.org/10.3389/fpls.2015.01077>
- Rigó G, Ayaydin F, Tietz O, et al (2013) Inactivation of Plasma Membrane–Localized CDPK-RELATED KINASE5 Decelerates PIN2 Exocytosis and Root Gravitropic Response in *Arabidopsis*. *Plant Cell* 25:1592–1608. <https://doi.org/10.1105/tpc.113.110452>
- Saha B, Borovskii G, Panda SK (2016) Alternative oxidase and plant stress tolerance. *Plant Signal Behav* 11:e1256530–e1256530. <https://doi.org/10.1080/15592324.2016.1256530>
- Saisho D, Nambara E, Naito S, et al (1997) Characterization of the gene family for alternative oxidase from *Arabidopsis thaliana*. *Plant Mol Biol* 35:585–596. <https://doi.org/10.1023/A:1005818507743>
- Salehi-Lisar SY, Bakhshayeshan-Agdam H (2016) Drought Stress in Plants: Causes, Consequences, and Tolerance. In: *Drought Stress Tolerance in Plants, Vol 1*. Springer International Publishing, Cham, pp 1–16
- Salone V, Rüdinger M, Polsakiewicz M, et al (2007) A hypothesis on the identification of the editing enzyme in plant organelles. *FEBS Lett* 581:4132–4138. <https://doi.org/10.1016/j.febslet.2007.07.075>
- Schertl P, Braun H-P (2014) Respiratory electron transfer pathways in plant mitochondria. *Front Plant Sci* 5:. <https://doi.org/10.3389/fpls.2014.00163>
- SCHMITZLINNEWEBER C, SMALL I (2008) Pentatricopeptide repeat proteins: a socket set for organelle gene expression. *Trends Plant Sci* 13:663–670. <https://doi.org/10.1016/j.tplants.2008.10.001>
- Sechet J, Roux C, Plessis A, et al (2015) The ABA-Deficiency Suppressor Locus HAS2 Encodes the PPR Protein LOI1/MEF11 Involved in Mitochondrial RNA Editing. *Mol Plant* 8:644–656. <https://doi.org/10.1016/j.molp.2014.12.005>
- Selinski J, Scheibe R, Day DA, Whelan J (2018) Alternative Oxidase Is Positive for Plant Performance. *Trends Plant Sci* 23:588–597. <https://doi.org/10.1016/j.tplants.2018.03.012>
- Sirichandra C, Gu D, Hu H-C, et al (2009) Phosphorylation of the Arabidopsis AtrbohF NADPH oxidase by OST1 protein kinase. *FEBS Lett* 583:2982–2986
- Small ID, Peeters N (2000) The PPR motif – a TPR-related motif prevalent in plant organellar proteins. *Trends Biochem Sci* 25:45–47. [https://doi.org/10.1016/S0968-0004\(99\)01520-0](https://doi.org/10.1016/S0968-0004(99)01520-0)

- Song S, Liu B, Song J, et al (2022) A molecular framework for signaling crosstalk between jasmonate and ethylene in anthocyanin biosynthesis, trichome development, and defenses against insect herbivores in *Arabidopsis*. *J Integr Plant Biol* 64:1770–1788
- Sperdoui I, Moustakas M (2012) Interaction of proline, sugars, and anthocyanins during photosynthetic acclimation of *Arabidopsis thaliana* to drought stress. *J Plant Physiol* 169:577–585. <https://doi.org/10.1016/j.jplph.2011.12.015>
- Szabados L, Kovács I, Oberschall A, et al (2002) Distribution of 1000 sequenced T-DNA tags in the *Arabidopsis* genome. *The Plant Journal* 32:233–242
- Szabados L, Saviouré A (2010) Proline: a multifunctional amino acid. *Trends Plant Sci* 15:89–97. <https://doi.org/10.1016/j.tplants.2009.11.009>
- Szekely G, Abraham E, Cseplo A, et al (2008) C si sz ar J Ayaydin F., Strizhov N., Jasik J., Schmelzer E., Koncz C., Szabados L. Duplicated P5CS genes of *Arabidopsis* play distinct roles in stress regulation and developmental control of proline biosynthesis. *Plant J* 53:11–28
- Takahashi F, Kuromori T, Sato H, Shinozaki K (2018) Regulatory Gene Networks in Drought Stress Responses and Resistance in Plants. pp 189–214
- Takahashi F, Kuromori T, Urano K, et al (2020) Drought Stress Responses and Resistance in Plants: From Cellular Responses to Long-Distance Intercellular Communication. *Front Plant Sci* 11:. <https://doi.org/10.3389/fpls.2020.556972>
- Takahashi F, Shinozaki K (2019) Long-distance signaling in plant stress response. *Curr Opin Plant Biol* 47:106–111. <https://doi.org/10.1016/j.pbi.2018.10.006>
- Tamasiga P, Ouassou E houssin, Onyeaka H, et al (2023) Forecasting disruptions in global food value chains to tackle food insecurity: The role of AI and big data analytics – A bibliometric and scientometric analysis. *J Agric Food Res* 14:100819. <https://doi.org/10.1016/j.jafr.2023.100819>
- Uhe P, Philip S, Kew S, et al (2018) Attributing drivers of the 2016 Kenyan drought. *International Journal of Climatology* 38:. <https://doi.org/10.1002/joc.5389>
- Unsold M, Marienfeld JR, Brandt P, Brennicke A (1997) The mitochondrial genome of *Arabidopsis thaliana* contains 57 genes in 366,924 nucleotides. *Nat Genet* 15:57–61
- Van Aken O (2021) Mitochondrial redox systems as central hubs in plant metabolism and signaling. *Plant Physiol* 186:36–52. <https://doi.org/10.1093/plphys/kiab101>
- Vanlerberghe GC, Martyn GD, Dahal K (2016) Alternative oxidase: a respiratory electron transport chain pathway essential for maintaining photosynthetic performance during drought stress. *Physiol Plant* 157:322–337. <https://doi.org/10.1111/ppl.12451>
- Wang R, Li X, Ma H, et al (2023) Persistent Meteorological Drought in the Yangtze River Basin during Summer–Autumn 2022: Relay Effects of Different Atmospheric Internal Variabilities. *Atmosphere (Basel)* 14:1402. <https://doi.org/10.3390/atmos14091402>
- Wang Y, Law SR, Ivanova A, et al (2014) The Mitochondrial Protein Import Component, TRANSLOCASE OF THE INNER MEMBRANE17-1, Plays a Role in Defining the Timing of Germination in *Arabidopsis*. *Plant Physiol* 166:1420–1435. <https://doi.org/10.1104/pp.114.245928>
- Wasternack C, Song S (2017) Jasmonates: biosynthesis, metabolism, and signaling by proteins activating and repressing transcription. *J Exp Bot* 68:1303–1321

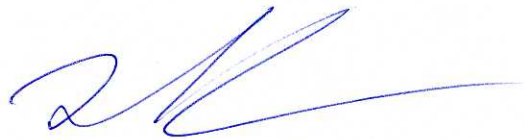
- Whelan J, Glaser* E (1997) Protein import into plant mitochondria. *Plant Mol Biol* 33:771–789
- Wickham H, Averick M, Bryan J, et al (2019) Welcome to the Tidyverse. *J Open Source Softw* 4:1686
- Wickham H, Wickham H (2016) Getting Started with ggplot2. *ggplot2: Elegant graphics for data analysis* 11–31
- Yaffe H, Buxdorf K, Shapira I, et al (2012) LogSpin: a simple, economical and fast method for RNA isolation from infected or healthy plants and other eukaryotic tissues. *BMC Res Notes* 5:45. <https://doi.org/10.1186/1756-0500-5-45>
- You J, Chan Z (2015) ROS Regulation During Abiotic Stress Responses in Crop Plants. *Front Plant Sci* 6:. <https://doi.org/10.3389/fpls.2015.01092>
- Yuan H, Liu D (2012) Functional disruption of the pentatricopeptide protein SLG1 affects mitochondrial RNA editing, plant development, and responses to abiotic stresses in *Arabidopsis*. *The Plant Journal* 70:432–444. <https://doi.org/10.1111/j.1365-313X.2011.04883.x>
- Zhang X, Zhang L, Dong F, et al (2001) Hydrogen Peroxide Is Involved in Abscisic Acid-Induced Stomatal Closure in *Vicia faba* . *Plant Physiol* 126:1438–1448. <https://doi.org/10.1104/pp.126.4.1438>
- Zhang Y, Lu C (2019) The Enigmatic Roles of PPR-SMR Proteins in Plants. *Advanced Science* 6:. <https://doi.org/10.1002/advs.201900361>
- Zhu Q, Dugardeyn J, Zhang C, et al (2014) The *Arabidopsis thaliana* RNA Editing Factor SLO2, which Affects the Mitochondrial Electron Transport Chain, Participates in Multiple Stress and Hormone Responses. *Mol Plant* 7:290–310. <https://doi.org/10.1093/mp/sst102>
- Zhu T, Zou L, Li Y, et al (2018) Mitochondrial alternative oxidase-dependent autophagy involved in ethylene-mediated drought tolerance in *Solanum lycopersicum*. *Plant Biotechnol J* 16:2063–2076. <https://doi.org/10.1111/pbi.12939>
- Zsigmond L, Rigó G, Szarka A, et al (2008) *Arabidopsis* PPR40 connects abiotic stress responses to mitochondrial electron transport. *Plant Physiol* 146:1721–1737
- Zsigmond L, Szepesi Á, Tari I, et al (2012) Overexpression of the mitochondrial PPR40 gene improves salt tolerance in *Arabidopsis*. *Plant Science* 182:87–93. <https://doi.org/10.1016/j.plantsci.2011.07.008>

10. List of publications: (MTMT: 10074888)

1. Mutation in Arabidopsis mitochondrial Pentatricopeptide repeat 40 gene affects tolerance to water deficit. **Kamal Kant**, Gábor Rigó, Dóra Faragó, Dániel Benyó, Roland Tengölics, László Szabados*, Laura Zsigmond*; *Planta*. (2024). **IF 4.3**
2. Mitochondrial complex I subunit NDUFS8.2 modulates responses to stresses associated with reduced water availability. Annabella Juhász-Erdélyi, Ildikó Valkai, Gábor Rigó, Agnes Szepesi, Dávid Alexa, **Kamal Kant**, Niklas Körber, Fabio Fiorani, László Szabados, Laura Zsigmond*; *Plant Physiology and Biochemistry*. (2024). **IF 5.6**

11. Declaration

I declare that the data used in the thesis written by **KAMAL KANT** reflect the contribution of the doctoral candidate to the article: Mutation in Arabidopsis mitochondrial Pentatricopeptide repeat 40 gene affects tolerance to water deficit. Kamal Kant, Gábor Rigó, Dóra Faragó, Dániel Benyó, László Szabados*, Laura Zsigmond*; *Planta*. (2024). The results reported in the Ph.D. thesis and the publication were not used to acquire any Ph.D. degree previously. I further declare that the candidate has made a significant contribution to the creation of the above-mentioned publication.



Zsigmond Laura, Ph.D.

Senior researcher, Institute of Plant Biology

HUN-REN Biological Research Centre Szeged

12. Supplementary data

Gene	Locus	Forward Primer (5'-3')	Reverse Primer (5'-3')	Reference
ACT2	<i>At3g18780</i>	GGTAACATTGTGCTCAGTGGTGG	AACGACCTTAATCTTCATGCTGC	(An et al. 1996)
UBC18	<i>At5g42990</i>	ACAGCAATGGACATATTTGTTAGA	TGATGCAGACTGAACTCACTGTC	(Ayaydin et al. 2015)
ZAT12	<i>At5g59820</i>	GACGCTTTGTCGTCTGGATT	GTGTCCTCCCAAAGCTTGTC	(Pérez-Salamó et al. 2014)
RD29A	<i>At5g52310</i>	ATCACTTGGCTCCACTGTTGTTTC	ACAAAACACACATAAACATCCAAAGT	(Pandey and Assmann 2004)
RAB18	<i>At5g66400</i>	CAGCAGCAGTATGACGAGTA	CAGTTCCAAAGCCTTCAGTC	(Pandey and Assmann 2004)
P5CS1	<i>At2g39800</i>	GGCAGATGGTCTTGTCTTAGAG	CACTACGGATGGCAAGTGAA	(Kant et al. 2024)
PDH1	<i>At3g30775</i>	GTCCTCTCTACCACACAAACTC	TGGACTCTTGGCATTTCCTAC	(Kant et al. 2024)
AOX1A	<i>At3g22370</i>	CTGGACCACGTTTGTTTC	ACACCCCAATAGCTCG	(Saisho et al. 1997)
AOX1D	<i>Atlg32350</i>	ATTGGAGGATTCAGGGGACA	CGTTCGGATAGGATTTTCTGG	(Kant et al. 2024)
AUX 1	<i>AT2G38120</i>	CTTTCCTCCTCTGCACATTCT	AAGAGTGGTTTTTGTCCGTTTG	(Rigó et al. 2013)
LAX3	<i>AT1G77690</i>	TGCTTACCTTTGCTCCTGCT	GTCCCATCCATCCTCCTAC	(Rigó et al. 2013)
EIN3	<i>AT3G20770</i>	AACTTTGGGATGGTTGCTAAAA	CTGGGACTTCTTCTTTGACAGG	Kant et al., 2024
WRKY30	<i>AT5G24110</i>	AGAGCGATGATTCCGATCAAG	CATCGTCCAGCGTTCTATCAA	(Besseau et al. 2012)
COI1	<i>AT2G39940</i>	TGATGATGTCATCGAGCAAG	ATGCTCTCTCGTCTCGGAAT	(Liu et al. 2016)
NPR1	<i>AT1G64280</i>	TTTACAGCAGCAGAGTGAGACC	AGCCAAATAGAGAACCTCCAACA	Kant et al., 2024